JCTC Journal of Chemical Theory and Computation

Article

pubs.acs.org/JCTC

Why is Benzene Soluble in Water? Role of OH/π Interaction in Solvation

Hideaki Takahashi,* Daiki Suzuoka, and Akihiro Morita

Department of Chemistry, Graduate School of Science, Tohoku University, Sendai, Miyagi 980-8578, Japan

Supporting Information

ABSTRACT: The XH/π interaction (X = C, N, or O) plays an essential role in a variety of fundamental processes in condensed phase, and it attracts broad interests in the fields of chemistry and biochemistry in recent years. This issue has a direct relevance to an intriguing phenomenon that a benzene molecule exhibits a negative solvation free energy of −0.87 kcal/mol in ambient water though it is a typical nonpolar organic solute. In this work, we developed a novel method to analyze the free energy $\delta\mu$ due to the electron density fluctuation of a solute in solution to clarify the mechanism responsible for the affinity of benzene to bulk water. Explicitly, the free energy $\delta\mu$ is decomposed into contributions from σ and π electrons in π-conjugated systems on the basis of the QM/MM method combined with a theory of solutions. With our analyses, the free energy $\delta\mu_\pi$ arising from the fluctuation of π electrons in benzene was obtained as −0.94 kcal/mol and found to be the major source of the affinity of benzene to water. Thus, the role of π electrons in hydration is quantified for the first time with our analyses. Our method was applied to phenyl methyl ether (PME) in water solution to examine the substituent effects of the electron donating group (EDG) on the hydration of a π-conjugated system. The delocalization effect of the π electrons on hydration was also investigated performing the decomposition analyses for ethene and 1,3-butadiene molecules in water solutions. It was revealed that the stabilization due to $\delta\mu_\pi$ for butadiene (−0.76 kcal/mol) is about three times as large as that for ethene (−0.26 kcal/mol), which suggests the importance of the delocalization effect of the π electrons in mediating the affinity to polar solvent.

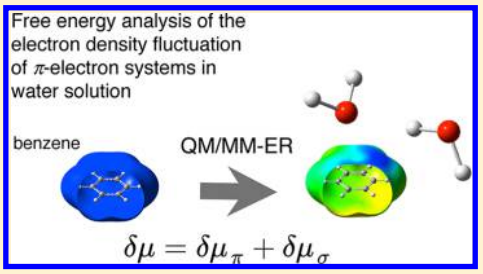

1. INTRODUCTION

Noncovalent interaction[1] is a major concern in physical chemistry of liquids, molecular aggregates, and biological systems because it plays a key role in a variety of fundamental processes such as solvation,[1−11] molecular stacking,[12,13] protein folding,[14−23] and molecular recognition.[12] Hydrogen bonding is, of course, a representative noncovalent interaction of primary importance. The major source of attractive forces in hydrogen bonding is the Coulomb interaction mediated by positively charged hydrogen atoms (protons) in molecules. Hydrogen bonding is a useful concept in interpreting the phenomena governed by electrostatic intermolecular forces. The detailed information on the interaction has been extensively studied through spectroscopic measurements and theoretical calculations, and the nature of the hydrogen bondings is well established.[12,24−26] Nonpolar interactions, on the other hand, have long been ascribed merely to the van der Waals interactions. It was suggested, however, in ref 14 that a considerable part of such weak interactions can be categorized into specific attractive interaction referred to as XH/π interactions (X = C, N, or O)[27] occurring between XH groups and π-electrons.[14−23] It is widely recognized that the XH/π interactions are commonly observed in proteins and important in organizing their structures and functionalities.[12−23,28] Thus, the XH/π interaction attracts broad interests in recent years in the fields of biochemistry as well as in chemistry. However, the energetics of the interaction in the context of condensed environment is not well examined nor understood on the quantitative basis.

Benzene is one of the fundamental building blocks in organic molecules, and therefore, the interaction of CH, NH, or OH bond with benzene[29] can be regarded as a typical XH/π interaction. For dimer systems, the interactions of OH or NH bonds with aromatic rings were studied performing high level ab initio calculations.[30] It was revealed for the dimer $H_2O-C_6H_6$ or $NH_3-C_6H_6$ that the induction effect due to the polarized σ bond of OH or NH on the aromatic ring governs the attractive interaction between the monomers though their absolute energies are much smaller than the conventional hydrogen bondings. The formation of such weak *hydrogen bond* between polarized benzene and the hydrogen of OH or NH is apparent in these static isolated dimers. Its role, however, in a condensed environment with thermal fluctuation remains to be unknown. The XH/π interaction of the solvent with the solute will be disturbed by competing attractive interaction among solvent molecules. These issues have direct relevance to a well-known fact that benzene is soluble in water (hydration free energy is negative: −0.87 kcal/mol) though it is a typical nonpolar organic molecule.[31−38] Although the affinity of benzene to a polar solvent is a clear indication of the importance of the OH/π interaction in a condensed phase,

Received: December 15, 2014
Published: February 5, 2015

DOI: 10.1021/ct501133u
J. Chem. Theory Comput. 2015, 11, 1181−1194

the origin of the affinity is not yet fully discussed on the basis of the quantum chemical analyses. Free energy of hydration of benzene should yield insight into the role of the XH/π interaction in the solvation process and in biological systems.

The major objective of the present work is to compute free energy contribution $\delta\mu_\pi$ due to the electron density fluctuation of π electrons in a benzene embedded in bulk water. For this purpose, we develop a novel computational technique to decompose the free energy $\delta\mu$ due to the electron density fluctuation utilizing our previous approach, referred to as QM/MM-ER,[39,40] which combines the quantum mechanical/molecular mechanical (QM/MM) method[2−4,7,10,11] with the theory of energy representation (ER).[41−44] The QM/MM-ER approach has been applied to various solution systems and its accuracy and reliability have been well established.[45−55] In a recent advance[56] in QM/MM-ER, we employed second order perturbation theory (PT2)[57−60] to compute free energy[40] due to the polarization of the wave functions of the QM solute in response to the dynamics of polar MM solvent. As will be discussed later, it is quite straightforward with the PT2 approach to decompose the polarization energy of the aromatic ring into the contributions from those of π and σ electrons. Our approach can take into consideration the polarization effects of the solute that cannot be described in principle in the mean-field approach such as polarizable continuum model (PCM).[61] We also note that the theory of energy representation,[41−43] a sort of a density functional theory of solutions,[62] offers an excellent theoretical framework well suited to our analyses. In addition, it is also possible to decompose the free energy $\delta\mu$ into the contributions due to the electronic polarization along the direction parallel and perpendicular to the molecular plane of benzene. These results provide quantitative discussions about the properties of OH/π interaction placed in a condensed environment. We perform the same analysis for another π-electron system to investigate the substituent effects on hydration. The role of the delocalization effect of the π electrons on hydration is also assessed extending the length of the π conjugation.

The organization of this paper is as follows. In the first part of the theoretical section, the concepts of static and dynamic electronic polarization are introduced to discuss the electron density fluctuation of π or σ electrons of a solute in solution. Then, we briefly review the perturbation approach[56] to compute the free energy $\delta\mu$ due to many-body interaction (dynamic polarization) within the framework of the QM/MM-ER method. The last of the theoretical section is devoted to describe the novel method to decompose the free energy $\delta\mu$ into the contributions from π and σ electrons in the solute. In the Computational Details section, numerical details are provided for the QM/MM simulations based on the Kohn−Sham density functional theory[63−65] utilizing the real-space grids.[66−70] In the final section, we present the results of our novel analyses and discuss the role of the OH/π interaction in the hydration processes.

2. THEORY AND METHODOLOGY

The theoretical basis within the framework of QM/MM-ER is presented for the free energy decomposition. In subsection 2.1, we first define the concept of static and dynamic polarizations of a solute in a solution. Then, the QM/MM simulation utilizing the second-order perturbation theory is briefly reviewed in subsection 2.2, which is followed by the description of the method to decompose the free energy $\delta\mu$ into contributions from σ and π electrons by means of the theory of solutions in subsections 2.3 and 2.4.

2.1. Static and Dynamic Polarization of a Solute in Solution. For the purpose of analyzing the role of the electron density fluctuation in solution, we introduce in this section the concepts of static and dynamic polarizations of a solute in solution. In the following, we assume a QM/MM system where a solute molecule is described with a method of quantum chemistry and solvent molecules are represented by classical force fields. For simplicity, it is also premised that configuration of the solute molecule is fixed during the simulation. Then, the total energy E_{tot} of the system is expressed by sum of three contributions,

$$E_{\mathrm{tot}} = E_{\mathrm{QM}} + E_{\mathrm{QM/MM}} + E_{\mathrm{MM}} \tag{1}$$

In eq 1, E_{QM} and E_{MM} are the energies of the QM and MM subsystems, respectively, and $E_{\mathrm{QM/MM}}$ is the interaction energy between two subsystems. In general, $E_{\mathrm{QM/MM}}$ consists of electrostatic and van der Waals interactions, thus,

$$E_{\mathrm{QM/MM}} = E^{\mathrm{ES}}_{\mathrm{QM/MM}} + E^{\mathrm{vdW}}_{\mathrm{QM/MM}} \tag{2}$$

$E^{\mathrm{ES}}_{\mathrm{QM/MM}}$ in eq 2 is the interaction between the solute and an electric field $\mathbf{V}_{\mathrm{pc}}$ yielded by point charges on MM solvent molecules. We split the potential $\mathbf{V}_{\mathrm{pc}}$ into static $\tilde{\mathbf{V}}_{\mathrm{pc}}$ and dynamic $\mathbf{V}_{\mathrm{pc}}[\mathbf{X}]-\tilde{\mathbf{V}}_{\mathrm{pc}}$ terms as

$$\mathbf{V}_{\mathrm{pc}}[\mathbf{X}] = \tilde{\mathbf{V}}_{\mathrm{pc}} + (\mathbf{V}_{\mathrm{pc}}[\mathbf{X}] - \tilde{\mathbf{V}}_{\mathrm{pc}}) \tag{3}$$

where notation $\mathbf{X}$ collectively represents the full coordinates of the solvent molecules at an instantaneous configuration. Note that $\tilde{\mathbf{V}}_{\mathrm{pc}}$ in eq 3 is independent of the configuration $\mathbf{X}$ and in this sense it is static, and of course, $\mathbf{V}_{\mathrm{pc}}[\mathbf{X}]-\tilde{\mathbf{V}}_{\mathrm{pc}}$ is responsible for the dynamic polarization of a solute. A natural and physically reasonable choice of $\tilde{\mathbf{V}}_{\mathrm{pc}}$ is to take the statistical average of $\mathbf{V}_{\mathrm{pc}}[\mathbf{X}]$ in solution, thus,

$$\tilde{V}_{\mathrm{pc}}(\mathbf{r}) = \frac{\int d\mathbf{X} V_{\mathrm{pc}}[\mathbf{X}](\mathbf{r})\exp(-\beta E_{\mathrm{tot}}[\mathbf{X}])}{\int d\mathbf{X}\exp(-\beta E_{\mathrm{tot}}[\mathbf{X}])} \tag{4}$$

where $\mathbf{r}$ denotes the position vector of the electron and β is the reciprocal of the Boltzmann constant k_{B} multiplied by temperature T. For the Hamiltonian $\mathbf{H}_0$ of the solute at isolation,we introduce a biased Hamiltonian $\mathbf{H}'_0$,

$$\mathbf{H}'_0 = \mathbf{H}_0 + \tilde{\mathbf{V}}_{\mathrm{pc}} \tag{5}$$

The static polarization of the solute molecule can, then, be given by solving the following Schrödinger equation for $\mathbf{H}'_0$,

$$\mathbf{H}'_0|\Psi'_0\rangle = E'_0|\Psi'_0\rangle \tag{6}$$

The electron density $\tilde{n}(\mathbf{r})$ associated with the static polarization is directly derived from the ground state wave function Ψ'_0 in eq 6. Assuming that E_0 is the ground state energy for $\mathbf{H}_0$, it is possible to define the distortion energy

$$E_{\mathrm{dist}} = \langle\Psi'_0|\mathbf{H}_0|\Psi'_0\rangle - E_0 = E'_0 - E_0 \tag{7}$$

of the solute under the influence of the static potential $\tilde{\mathbf{V}}_{\mathrm{pc}}$. The dynamic polarization of the solute is due to the residual potential $\mathbf{V}'_{\mathrm{pc}}[\mathbf{X}] \equiv \mathbf{V}_{\mathrm{pc}}[\mathbf{X}] - \tilde{\mathbf{V}}_{\mathrm{pc}}$, which is dependent on the solvent configuration. Thus, the free energy $\delta\mu$ of our interest arises from the fluctuation of the electron density $n[\mathbf{X}]$ around the fixed distribution $\tilde{n}$ that corresponds to the mean field $\tilde{\mathbf{V}}_{\mathrm{pc}}$. It is worthy of note that the polarizable continuum model (PCM)[61] and reference interaction site model coupled with

DOI: 10.1021/ct501133u
J. Chem. Theory Comput. 2015, 11, 1181−1194

SCF procedures (RISM-SCF)[71,72] are the methods to realize the *static* polarization of a solute using the "mean-field" approach on the basis of the fundamental electromagnetism and the theory of solutions, respectively. Hence, these approaches cannot take into consideration the dynamic polarization in principle.

2.2. Perturbation Approach to QM/MM Method. In this section, we review the method to treat dynamic polarization of a solute with second-order perturbation approach.[56−60] For our present purpose, we take the biased Hamiltonian $\mathbf{H}_0'$ defined by eq 5 as a zeroth-order Hamiltonian for the perturbation expansion. Then, the Hamiltonian $\mathbf{H}$ for the solute in solution can be represented as

$$\mathbf{H} = \mathbf{H}_0' + \mathbf{V}_{\mathrm{pc}}'[\mathbf{X}] = \mathbf{H}_0' + (\mathbf{V}_{\mathrm{pc}}[\mathbf{X}] - \tilde{\mathbf{V}}_{\mathrm{pc}}) \tag{8}$$

We note that $\mathbf{H}_0'$ is independent of $\mathbf{X}$ and only the term $\mathbf{V}_{\mathrm{pc}}'[\mathbf{X}]$ in eq 8 is responsible for the deviation of solute's electron density n from its average distribution $\tilde{n}$. Applying the perturbation theory with respect to the potential $\mathbf{V}_{\mathrm{pc}}'[\mathbf{X}]$, we have expansion series,

$$E_{\mathrm{QM}} + E_{\mathrm{QM/MM}}^{\mathrm{ES}} = E'^{(0)} + E'^{(1)} + E'^{(2)} + \cdots \tag{9}$$

The zeroth-order term $E'^{(0)}$ in eq 9 is the ground state energy for the Hamiltonian $\mathbf{H}_0'$ and equals to E'_0 in eq 6. The first order term $E'^{(1)}$ is the electrostatic interaction between $\mathbf{V}_{\mathrm{pc}}'$ and unperturbed solute with density $\tilde{n}$, which is given by

$$E'^{(1)} = \int \mathrm{d}\mathbf{r}\tilde{n}(\mathbf{r})V_{\mathrm{pc}}'[\mathbf{X}](\mathbf{r}) + \sum_{k\in\mathrm{QM}} Z_k \cdot V_{\mathrm{pc}}'[\mathbf{X}](\mathbf{R}_k) \tag{10}$$

In eq 10 Z_k and $\mathbf{R}_k$ stand for the nuclear charge and the position vector of the kth atom in the QM region, respectively. The zeroth and first order terms in the perturbation series are responsible for the two-body interaction between solute and solvent because the electron density of the solute is fixed at $\tilde{n}$ regardless of the configuration $\mathbf{X}$.

Provided that the zeroth-order wave function Ψ_0' is represented with a single determinant by means of Kohn−Sham density functional theory (KS-DFT) or Hartree−Fock approach, the second order term $E'^{(2)}$ in the expansion of eq 9 can be expressed as

$$E'^{(2)} = \sum_i^{\mathrm{occ}} \sum_a^{\mathrm{vir}} \frac{1}{\varepsilon_i'^{(0)} - \varepsilon_a'^{(0)}} |\langle \varphi_i'^{(0)}|\mathbf{V}_{\mathrm{pc}}'[\mathbf{X}]|\varphi_a'^{(0)}\rangle|^2 \tag{11}$$

where $\{\varphi_i'^{(0)}\}$ and $\{\varepsilon_i'^{(0)}\}$ are the sets of eigenfunctions and eigenvalues for the reference Hamiltonian $\mathbf{H}_0'$. $E'^{(2)}$ in eq 9 describes the energy due to dynamic polarization of the solute and is the source of the many-body interaction in the QM/MM system. For later references, it is also helpful to provide the quantity $n'^{(2)}(\mathbf{r})$, referred to as polarization density,[56]

$$n^{(2)}[\mathbf{X}](\mathbf{r}) = \sum_i^{\mathrm{occ.}} \sum_a^{\mathrm{vir.}} \frac{1}{\varepsilon_i'^{(0)} - \varepsilon_a'^{(0)}} \langle \varphi_i'^{(0)}|\mathbf{V}_{\mathrm{pc}}'[\mathbf{X}]|\varphi_a'^{(0)}\rangle \times \varphi_a'^{(0)*}(\mathbf{r})\varphi_i'^{(0)}(\mathbf{r}) \tag{12}$$

which describes the leading contribution to the density shift of the solute due to the fluctuating potential $\mathbf{V}_{\mathrm{pc}}'[\mathbf{X}]$. In the following discussion, we consider the polarization energy due to density fluctuation up to the second order in the perturbation expansion (PT2) for computational convenience. The adequacy of the truncation in the evaluation of the free energy was fully examined in our previous paper.[56]

2.3. QM/MM-ER Method Combined with PT2 Approach. This subsection serves as a brief review for the QM/MM-ER method[39,40] combined with the second-order perturbation approach[40,56] with a focus on the treatment of the free energy contribution $\delta\mu$ due to the electron density fluctuation. Within the framework of the QM/MM approach, the solvation free energy $\Delta\mu$ of the solute is exactly expressed as

$$\exp(-\beta\Delta\mu) = \frac{\int \mathrm{d}\mathbf{X}\exp[-\beta(E_{\mathrm{QM}}[\mathbf{X}] - E_0 + E_{\mathrm{QM/MM}}(n[\mathbf{X}], \mathbf{X}) + E_{\mathrm{MM}}[\mathbf{X}])]}{\int \mathrm{d}\mathbf{X}\,\exp[-\beta(E_{\mathrm{MM}}[\mathbf{X}])]} \tag{13}$$

Using the PT2 approximation introduced in the previous section, free energy $\Delta\mu$ of eq 13 can be approximated as

$$\exp(-\beta\Delta\mu) \cong \{\int \mathrm{d}\mathbf{X}\,\exp[-\beta(E'^{(0)} + E'^{(1)} + E'^{(2)} - E_0 + E_{\mathrm{QM/MM}}^{\mathrm{vdW}}[\mathbf{X}] + E_{\mathrm{MM}}[\mathbf{X}])]\}/\{\int \mathrm{d}\mathbf{X}\,\exp[-\beta(E_{\mathrm{MM}}(\mathbf{X}))]\} \tag{14}$$

where the *dynamic* potential $\mathbf{V}_{\mathrm{pc}}'[\mathbf{X}]$ is regarded as a perturbation. In the method of the QM/MM-ER approach, the free energy $\Delta\mu$ is formally decomposed into two contributions $\Delta\bar{\mu}$ and $\delta\mu$, thus,

$$\exp(-\beta\Delta\mu) = \exp(-\beta\Delta\bar{\mu})\exp(-\beta\delta\mu) \cong \frac{\int d\mathbf{X}\,\exp[-\beta(E'^{(0)} + E'^{(1)} - E_0 + E_{\mathrm{QM/MM}}^{\mathrm{vdW}}[\mathbf{X}] + E_{\mathrm{MM}}(\mathbf{X}))]}{\int d\mathbf{X}\,\exp[-\beta(E_{\mathrm{MM}}(\mathbf{X}))]} \cdot \frac{\int d\mathbf{X}\,\exp[-\beta(E'^{(0)} + E'^{(1)} + E'^{(2)} - E_0 + E_{\mathrm{QM/MM}}^{\mathrm{vdW}}[\mathbf{X}] + E_{\mathrm{MM}}(\mathbf{X}))]}{\int d\mathbf{X}\,\exp[-\beta(E'^{(0)} + E'^{(1)} - E_0 + E_{\mathrm{QM/MM}}^{\mathrm{vdW}}[\mathbf{X}] + E_{\mathrm{MM}}(\mathbf{X}))]} \tag{15}$$

As described in the preceding section, the energy $E'^{(0)} + E'^{(1)} - E_0$ corresponds to the two-body electrostatic interaction between solute and solvent, while $E'^{(2)}$ comes from the dynamic polarization of the QM solute. Thus, the free energy $\Delta\bar{\mu}$ in eq 15 constitutes the solvation free energy of the solute with the electron density fixed at $\tilde{n}$, while $\delta\mu$ represents the contribution due to electron density fluctuation around the distribution $\tilde{n}$ in response to the solvent dynamics.

We provide here the outline to calculate $\Delta\bar{\mu}$ with the method of QM/MM-ER. The distribution function $\rho(\varepsilon)$ is constructed for the two-body interaction energies ε between a solute and solvent molecules in a solution system, while the distribution $\rho_0(\varepsilon)$ and the correlation matrix $\chi_0(\varepsilon, \varepsilon')$ are yielded in the pure solvent system.[39,41−43] Then, these distribution functions of the pair potential serve as fundamental variables for an approximate functional to evaluate free energy $\Delta\bar{\mu}$ on the basis of the density functional theory of solutions. The explicit definitions for the energy distributions $\rho(\varepsilon)$, $\rho_0(\varepsilon)$, and $\chi_0(\varepsilon, \varepsilon')$ are presented in ref 39. The accuracy and the efficiency of the method to compute two-body contribution $\Delta\bar{\mu}$ were well established in the previous works.[44−55] Because the major concern of the present work is the electron density fluctuation of a solute, details for the method to compute $\Delta\bar{\mu}$ will not be described in this article. We refer the readers to the related papers.[39,41−43]

The residual contribution $\delta\mu$ is to be evaluated using another free energy functional in the framework of the QM/MM-ER method.[40] To compute $\delta\mu$ utilizing the method of energy representation coupled with PT2, we introduce a new energy coordinate η, which describes the energy shift due to the

DOI: 10.1021/ct501133u
J. Chem. Theory Comput. 2015, 11, 1181−1194

dynamic electronic polarization of the solute, that is, $E'^{(2)}$ in eq 11 is taken as the energy coordinate η:

$$\eta = E'^{(2)}[\mathbf{X}] \tag{16}$$

Then, the distribution functions $P(\eta)$ and $P_0(\eta)$ are constructed in solution and reference systems, respectively, thus,

$$\begin{aligned} P(\eta) &= \{ \int d\mathbf{X}\delta(\eta - E'^{(2)})\exp[-\beta(E'^{(0)} + E'^{(1)} + E'^{(2)} \\ &\quad - E_0 + E^{vdW}_{QM/MM}[\mathbf{X}] + E_{MM}[\mathbf{X}])]\} \\ &\quad /\{ \int d\mathbf{X}\exp[-\beta(E'^{(0)} + E'^{(1)} + E'^{(2)} - E_0 \\ &\quad + E^{vdW}_{QM/MM}[\mathbf{X}] + E_{MM}[\mathbf{X}])]\} \\ &= \{ \int d\mathbf{X}\delta(\eta - E'^{(2)})\exp[-\beta(E'^{(1)} + E'^{(2)} \\ &\quad + E^{vdW}_{QM/MM}[\mathbf{X}] + E_{MM}[\mathbf{X}])]\} \\ &\quad /\{ \int d\mathbf{X}\exp[-\beta(E'^{(1)} + E'^{(2)} + E^{vdW}_{QM/MM}[\mathbf{X}] \\ &\quad + E_{MM}[\mathbf{X}])]\} \end{aligned} \tag{17}$$

$$\begin{aligned} P_0(\eta) &= \frac{\int d\mathbf{X}\delta(\eta - E'^{(2)})\exp[-\beta(E'^{(0)} + E'^{(1)} - E_0 + E^{vdW}_{QM/MM}[\mathbf{X}] + E_{MM}[\mathbf{X}])]}{\int d\mathbf{X}\exp[-\beta(E'^{(0)} + E'^{(1)} - E_0 + E^{vdW}_{QM/MM}[\mathbf{X}] + E_{MM}[\mathbf{X}])]} \\ &= \frac{\int d\mathbf{X}\delta(\eta - E'^{(2)})\exp[-\beta(E'^{(1)} + E^{vdW}_{QM/MM}[\mathbf{X}] + E_{MM}[\mathbf{X}])]}{\int d\mathbf{X}\exp[-\beta(E'^{(1)} + E^{vdW}_{QM/MM}[\mathbf{X}] + E_{MM}[\mathbf{X}])]} \end{aligned} \tag{18}$$

In the construction of these functions, we dropped the terms $E'^{(0)}$ and E_0 both in the denominator and numerator because they are independent of the coordinate $\mathbf{X}$. It can be readily realized in eqs 17 and 18 that the QM solute fully couples with the solvent in the solution system, while in the reference system it interacts with the solvent with a two-body potential. With these distributions $P(\eta)$ and $P_0(\eta)$, it is possible to formulate exactly the free energy $\delta\mu$ as[40]

$$\delta\mu = \int \left(k_B T \ln\left(\frac{P(\eta)}{P_0(\eta)}\right) + \eta \right) W(\eta) d\eta = \int R(\eta) W(\eta) d\eta \tag{19}$$

$W(\eta)$ in eq 19 can be chosen arbitrarily as long as it is normalized.[73] Of course, an elaborate construction of $W(\eta)$ will reduce the statistical errors in the numerical computation of $\delta\mu$.

2.4. Decomposition of the Free Energy $\delta\mu$. To analyze the solvation free energy $\delta\mu$, we formulate here the method to decompose the free energy $\delta\mu$ into contributions $\delta\mu_\pi$ and $\delta\mu_\sigma$ ($\delta\mu = \delta\mu_\pi + \delta\mu_\sigma$) due, respectively, to π and σ electrons in an aromatic ring immersed in a solvent. It is quite straightforward to decompose the PT2 energy $E'^{(2)}$ in eq 11 into two contributions, which reads

$$\begin{aligned} E'^{(2)} &= E'^{(2)}_\pi + E'^{(2)}_\sigma = \left(\sum_{i\in\pi}^{occ} + \sum_{i\in\sigma}^{occ}\right) \\ &\quad \times \sum_a^{vir} \frac{1}{\varepsilon_i'^{(0)} - \varepsilon_a'^{(0)}} |\langle \varphi_i'^{(0)} | V'_{pc}[\mathbf{X}] | \varphi_a'^{(0)} \rangle|^2 \end{aligned} \tag{20}$$

Clearly, the term $E'^{(2)}_\pi$ defined in eq 20 represents the energy shift due to the polarization of π electrons and the term $E'^{(2)}_\sigma$ describes that of σ electrons. In terms of the spatial distribution functions $\rho(\mathbf{X})$ of the configuration $\mathbf{X}$, the free energy $\delta\mu$ in eq 19 can be expressed by sum of two contributions $\delta\mu_\pi$ and $\delta\mu_\sigma$ on the basis of the Kirkwood's charging equation,[62]

$$\begin{aligned} \delta\mu = \delta\mu_\pi + \delta\mu_\sigma &= \int_0^1 d\lambda \int d\mathbf{X}\rho(\mathbf{X};\lambda)\frac{d}{d\lambda}E'^{(2)}_{\pi,\lambda}[\mathbf{X}] \\ &\quad + \int d\lambda \int d\mathbf{X}\rho(\mathbf{X};\lambda)\frac{d}{d\lambda}E'^{(2)}_{\sigma,\lambda}[\mathbf{X}] \end{aligned} \tag{21}$$

λ in eq 21 denotes the coupling parameter describing the degree of electronic polarization of the solute interacting with the solvent. At $\lambda = 0$, the solute electron density is fixed at the distribution $\tilde{n}$ while at $\lambda = 1$ solute electrons fully couple with fluctuating electric field $\mathbf{V}'_{pc}[\mathbf{X}]$. $\rho(\mathbf{X};\lambda)$ represents the distribution of solvent configuration $\mathbf{X}$ at a coupling parameter λ. The second-order terms $E'^{(2)}_\pi$ and $E'^{(2)}_\sigma$ are, of course, dependent on the coupling parameter λ as well as $\mathbf{X}$. We note that eq 21 is expressed in terms of the distribution functions ρ as functions of the spatial coordinate $\mathbf{X}$ which consists of huge number of variables. Hence, it is not feasible to treat eq 21 with a numerical approach. As shown in the Appendix, however, it is also possible to formulate it using distribution functions of the polarization energy η of one dimension. For the free energy $\delta\mu_\pi$, for instance, we have the following Kirkwood's charging equation in terms of the energy distribution function $P_\pi(\eta;\lambda)$,

$$\delta\mu_\pi = \int_0^1 d\lambda \int d\eta P_\pi(\eta;\lambda)\frac{d}{d\lambda}E'^{(2)}_{\pi,\lambda}(\eta) \tag{22}$$

The free energy $\delta\mu_\sigma$ can also be given in the form parallel to eq 22. Introducing the indirect part $\omega_\pi(\eta;\lambda)$ of the solute−solvent interaction of mean force, the free energy $\delta\mu_\pi$ in eq 22 can be formulated as

$$\begin{aligned} \delta\mu_\pi &= -k_B T \int d\eta [((P_\pi(\eta) - P_{0,\pi}(\eta)) + \beta\omega_\pi(\eta)P_\pi(\eta) \\ &\quad - \beta \int_0^1 d\lambda \omega_\pi(\eta;\lambda)(P_\pi(\eta) - P_{0,\pi}(\eta)))] \end{aligned} \tag{23}$$

$P_\pi(\eta)$ and $P_{0,\pi}(\eta)$ are, respectively, the distribution functions of $E'^{(2)}_\pi$ in solution and reference systems and defined as

$$\begin{aligned} P_\pi(\eta) \equiv P_\pi(\eta;1) &= \{ \int d\mathbf{X}\delta(\eta - E^{(2)}_\pi) \\ &\quad \times \exp\{-\beta(E'^{(1)} + E'^{(2)} + E^{vdW}_{QM/MM}[\mathbf{X}] + E_{MM}[\mathbf{X}])\}\} \\ &\quad /\{ \int d\mathbf{X}\exp\{-\beta(E'^{(1)} + E'^{(2)} + E^{vdW}_{QM/MM}[\mathbf{X}] + E_{MM}[\mathbf{X}])\}\} \end{aligned} \tag{24}$$

$$\begin{aligned} P_{0,\pi}(\eta) \equiv P_\pi(\eta;0) &= \frac{\int d\mathbf{X}\delta(\eta - E^{(2)}_\pi)\exp\{-\beta(E'^{(1)} + E^{vdW}_{QM/MM}[\mathbf{X}] + E_{MM}[\mathbf{X}])\}}{\int d\mathbf{X}\exp\{-\beta(E'^{(1)} + E^{vdW}_{QM/MM}[\mathbf{X}] + E_{MM}[\mathbf{X}])\}} \end{aligned} \tag{25}$$

In eqs 24 and 25 we dropped the energy terms $E'^{(0)}$ and E_0 since they are independent of $\mathbf{X}$. The indirect part $\omega_\pi(\eta;\lambda)$ in eq 23 is expressed in terms of the energy distribution functions,

$$\omega_\pi(\eta;\lambda) = -k_B T \log\left(\frac{P_\pi(\eta;\lambda)}{P_\pi(\eta;0)}\right) - \eta \tag{26}$$

Specifically $\omega_\pi(\eta)$ in eq 23 stands for $\omega_\pi(\eta;1)$. The integration of $\omega_\pi(\eta;\lambda)$ with respect to λ is performed with Percus−Yevick (PY) and Hypernetted Chain (HNC) approximations,[39,42,62] that is,

DOI: 10.1021/ct501133u
J. Chem. Theory Comput. 2015, 11, 1181−1194

$$\beta \int_0^1 \omega_\pi(\eta;\lambda)\mathrm{d}\lambda = \begin{cases} \beta\omega_\pi(\eta) + 1 + \dfrac{\beta\omega_\pi(\eta)}{\exp(-\beta\omega_\pi(\eta)) - 1} & (\omega_\pi(\eta) \le 0) \\ \dfrac{1}{2}\beta\omega_\pi(\eta) & (\omega_\pi(\eta) \ge 0) \end{cases} \tag{27}$$

In eq 27, the PY approximation is used to integrate the favorable region ($\omega_\pi(\eta) \le 0$) while HNC is utilized for the unfavorable region ($\omega_\pi(\eta) \ge 0$). We note that only the distribution functions at $\lambda = 0$ and 1 are needed to evaluate the integration of $\omega_\pi(\eta;\lambda)$ with eq 27. The equations parallel to eqs 22−27 hold for the free energy $\delta\mu_\sigma$ and the related distribution functions. The polarization of π electrons, of course, couples with that of σ electrons, and the indirect part $\omega_\pi(\eta;\lambda)$ of the mean potential carries the information on the correlation between these two polarization energies. Due to the correlation between the fluctuations of π and σ electrons, the free energy contributions $\delta\mu_\pi$ and $\delta\mu_\sigma$ can only be evaluated with approximate functionals. This makes a contrast to the whole free energy $\delta\mu$, which can be computed with an exact functional given by eq 19. We stress that it is the mean potential $\omega_\pi(\eta;\lambda)$, which enables ones to decompose free energy in a formally natural manner. The validity of the decomposition of the free energy can be examined comparing the value $\delta\mu$ with the sum of the constituent free energies $\delta\mu_\pi$ and $\delta\mu_\sigma$ Thus, a reasonable decomposition of the free energy $\delta\mu$ was made possible into the contributions due to π and σ electrons by virtue of the density functional theory of solutions coupled with the perturbation theory for electronic energy.

3. COMPUTATIONAL DETAILS

To analyze the role of OH/π interaction in hydration process, we consider in this article infinitely dilute binary solutions where benzene (C_6H_6), phenyl methyl ether ($C_6H_5OCH_3$), ethene (C_2H_4), and 1,3-butadiene (C_4H_6) are immersed in water solvents, respectively. Here, we address the numerical details about the free energy calculations. The first subsection provides the method to determine the structures of the solute molecules in water solution. Details are described in the second subsection for the construction of the unperturbed wave functions for the QM solute employed in the QM/MM-PT2 simulations. Setups for the QM/MM simulations are given in the third subsection. Finally, the fourth subsection is devoted to describe the statistical details for the construction of the energy distribution functions.

3.1. Geometry Optimizations. Geometries of the solute molecules were determined utilizing the Kohn−Sham density functional theory (KS-DFT)[63−65] with aug-cc-pVDZ basis set[74] in Gaussian 09 program package,[75] where electronic exchange and correlation energies were evaluated using B3LYP functional.[76−78] To mimic the influences of the water solvent on the geometries of the solutes, we employed the polarizable continuum model (PCM).[61] Because the geometries of larger systems will be affected seriously by the solvent, the solvent effects on the structures for larger solutes should be examined using some explicit solvent models. The Cartesian coordinates for each solute are summarized in the table in Supporting Information.

3.2. Real-Space Grid DFT and PT2 Calculations. Prior to the QM/MM simulations combined with PT2 approach, it is necessary to construct the zeroth order wave functions $\{\varphi_i'^{(0)}\}$ and eigenvalues $\{\varepsilon_i'^{(0)}\}$ for the biased Hamiltonian $\mathbf{H}_0'$ defined in eq 5 that includes the average electric field $\tilde{\mathbf{V}}_{pc}$ formed by solvent.[56] The wave functions $\{\varphi_i'^{(0)}\}$ for each solute molecule were obtained through an SCF procedure using the KS-DFT code in the QM/MM program developed by Takahashi et al.[68−70] In the summations of eqs 11, 12, and 20, we considered the virtual orbitals of which eigenvalues were less than 0.2 au This cutoff energy is the same as that adopted in the previous work and proved to be adequate. The notable feature of our DFT code is that one-electron wave functions as well as operators for the QM region are represented using real-space grids (RSG) uniformly distributed over a rectangular box. The kinetic energy operators for electrons were approximated by fourth-order finite difference method proposed by Chelikowsky et al.[66,67] and the interaction between electrons and nuclei were evaluated by pseudopotentials in a fully nonlocal form developed by Kleinmann and Bylander.[79] In the present simulations, we employed a cubic QM cell that had 64 grid points along each axis. The grid spacing h was set at 0.152 Å, which led to the QM cell size of L_{QM} = 9.71 Å. To realize the rapid behaviors of the wave functions near the atomic core regions, we introduced double grids,[80] for which the width of the dense grid was set at $h/5$. The accuracy and adequacy of our real-space grid DFT were fully examined in our previous works.[39,40,45−55,68−70] Using the zeroth-order wave functions $\{\varphi_i'^{(0)}\}$ and eigenvalues $\{\varepsilon_i'^{(0)}\}$, we computed the PT2 forces acting on the interaction sites on the solvent molecules in the subsequent MD simulations, which served to construct the energy distribution functions defined by eqs 24 and 25. The PT2 forces due to the polarized solute were calculated using eq 20 of ref 56. The geometries and positions of the solutes were being fixed during these QM/MM-PT2 simulations. Hence, it was not necessitated to update the wave functions $\{\varphi_i'^{(0)}\}$ and eigenvalues $\{\varepsilon_i'^{(0)}\}$ at each MD step once they were constructed before simulations.

3.3. QM/MM Simulations. The simulation cell for QM/MM combined with PT2 was prepared with the following procedure. First, the MM subsystem was constructed by embedding 500 solvent water molecules within a cubic simulation box with periodic boundary conditions.[81,82] The SPC/E model[83] was adopted to represent the MM water molecule. The size L_{MM} of the MM cell was, then, adjusted to reproduce the ambient water density 1.0 g/cm^3, which led to the size of L_{MM} = 24.6 Å. To insert a QM solute into the simulation cell, we eliminated solvent molecules whose total volume amounts approximately to that of the solute. The molecular volumes for the solutes were those given in the standard PCM calculations in Gaussian 09 (B3LYP/aug-cc-pVDZ). As a result, the number of water molecules in the simulation box was reduced to 496−498 depending on the size of the solutes. The constant-NVT molecular dynamics (MD) simulation was performed by rescaling velocities[81,82] to set temperature T at 300 K. The equation of motion was solved numerically by the leap-flog algorithm[81,82] with time step 1 fs. The solvent−solvent Coulombic interactions were calculated by the Ewald method,[81,82] while the QM-MM electrostatic interaction was evaluated by the bare form of $1/r$ with the minimum image convention. The cut off distance of the potential was set at half of the box length for the Lennard-Jones (LJ) interaction and for the real-space part of the Ewald interaction. To evaluate the van der Waals interaction energy $E_{QM/MM}^{vdW}$, we adopted the GROMOS 43A1 force field[84] for benzene and OPLS-AA[85] for the other solute molecules. The long-range correction $\Delta\bar{\mu}_{1c}$, which is the free energy contribution due to the LJ interaction from the region outside

DOI: 10.1021/ct501133u
J. Chem. Theory Comput. 2015, 11, 1181−1194

the cut off distance, was estimated with an equation in section 2.8 of ref 81.

The average potential $\tilde{\mathbf{V}}_{pc}$ of eq 4 for each solute was yielded through an ordinary 500 ps QM/MM simulation where an SCF procedure for KS-DFT with BLYP functional was carried out at each MD step. The computational setup for this simulation was the same as that for QM/MM-PT2 calculation noted above. The zeroth-order wave functions $\{\varphi_i'^{(0)}\}$ were, then, constructed for the biased Hamiltonian $\mathbf{H}_0+\tilde{\mathbf{V}}_{pc}$. The long-range correction to the exchange energy is, in general, crucial for the accurate description of the polarization of the π-conjugated systems. In our systems, however, the lengths of the π-conjugations are so short that they can be managed adequately with ordinary GGA(generalized gradient approximation) functional.

For readers' references, the potential energy curves calculated with the QM/MM-PT2 method are presented for the benzene-water dimers in in-plane and on-top configurations in Figures 1 and 2 in Supporting Information, respectively. The curves are also compared with those obtained using other theoretical methods as well as the ordinary QM/MM potentials.

3.4. Energy Distribution Functions. As shown in eq 15, the total solvation free energy $\Delta\mu$ is decomposed into the contributions of $\Delta\bar{\mu}$ and $\delta\mu$, which are computed separately in the QM/MM-ER approach. By means of the functional defined by eq 19, we computed the free energy $\delta\mu$ due to electron density fluctuation of each solute around the fixed distribution $\tilde{n}$. To do this, the energy distribution functions $P(\eta)$ and $P_0(\eta)$ defined by eqs 17 and 18 were constructed through 200 ps simulations of QM/MM-PT2 for both solution and reference systems. The free energy component $\delta\mu_\pi$ expressed in eq 23 for π electrons was also evaluated using approximation of eq 27, which employs distribution functions $\rho^e_\pi(\eta)$ and $\rho^e_{0,\pi}(\eta)$ in eqs 24 and 25. We also carried out QM/MM-PT2 simulations for 200 ps to yield these distributions. The free energy component $\delta\mu_\sigma$ for σ electrons was also computed with the same procedure as π electrons. In the computation of the solvation free energies, we neglected the free energies of molecular vibrations because these contributions will reasonably cancel those in the gas phase when one evaluates the solvation free energies. We note, however, the molecular vibration will slightly give rise to additional electronic fluctuation of the solute in solution.

To compute free energy contribution $\Delta\bar{\mu}$ due to two-body interaction between solute and solvent with the method of energy representation, the distribution functions $\rho(\varepsilon)$ and $\rho_0(\varepsilon)$ for pair interaction potential ε were constructed for solution and pure solvent systems, respectively. The correlation matrices $\chi_0(\varepsilon, \varepsilon')$ for the pair potential were also produced in the pure solvent systems. 200 ps simulation was devoted for the solution system for each solute. The simulation for the pure solvent system was carried out for 100 ps, in which 1000-times random insertions of the solute into the solvent were performed at every 100 steps (100 fs). This led to production of 10^6 configurations in total. For the constructions of the distribution functions for $\Delta\bar{\mu}$, we considered the solvent molecules of which mass centers were located within a sphere Ω of radius 11 Å. The center of sphere Ω was placed at the mass center of each solute.

4. RESULTS AND DISCUSSIONS

4.1. Role of Static Polarization in Hydration of Benzene. Shown in Figure 1 are two-dimensional contour maps of the average electrostatic potential $\tilde{\mathbf{V}}_{pc}$ formed by the solvent around benzene. Potentials $\tilde{\mathbf{V}}_{pc}$ on the molecular plane (upper) and on the symmetry plane (lower) perpendicular to the molecular plane are shown in the figure. The potential on the molecular plane is characterized by the well-defined structure of the positive potential wall surrounding the benzene ring. In contrast, it is found in the lower figure that a distinct negative region of potential appears above the benzene ring implying formation of a hydrogen bond between water OH and the benzene ring. This result is completely consistent with an experimental observation that revealed the formation of the hydrogen bonds between water molecules positioned above the benzene ring and the benzene which acts as a proton acceptor. The computations based on the accurate ab initio molecular orbitals theory in ref 30 also support our results. According to the MP2/cc-pVQZ calculations with BSSE corrections for a water−benzene dimer, the binding energy of the configuration where the OH bond is pointing to the center of the aromatic ring was evaluated to be as much as 3.13 kcal/mol at the optimum distance.

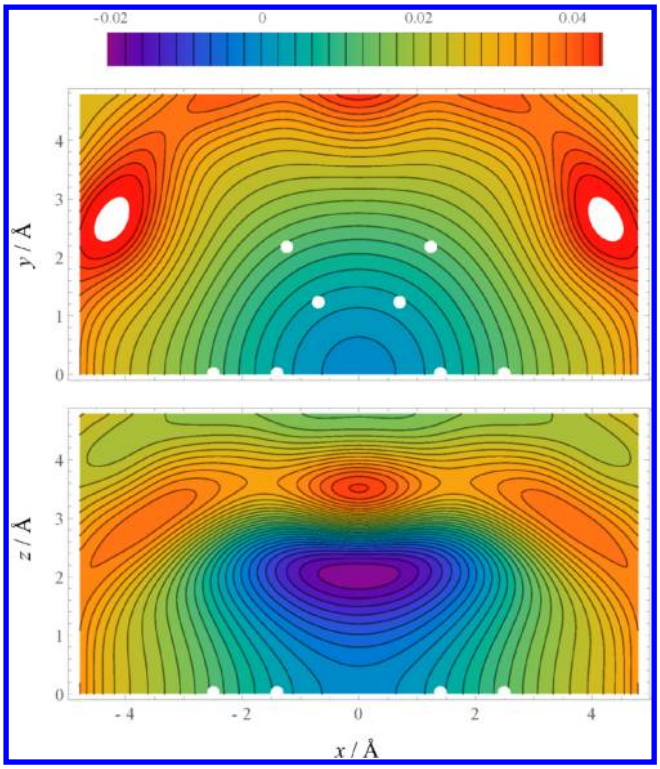

Figure 1. Contour plots of the average electrostatic potential $\tilde{\mathbf{V}}_{pc}$ for benzene. The potential values in legend are in au. The molecular plane of benzene is aligned parallel to the *xy* plane, where two carbon atoms and the center of the aromatic ring are placed on the *x* axis. The upper figure shows the potential on the molecular plane and the lower one is for the potential on the *xz* plane. Only the half regions with respect to the molecular symmetry planes are drawn and the positions of C and H atoms are depicted with white dots in the figure. For the symmetry of benzene $\tilde{\mathbf{V}}_{pc}$ is yielded by taking the average of the raw data of $\tilde{\mathbf{V}}_{pc}$ with respect to the three symmetry planes which are perpendicular to the *x*, *y*, and *z* axes.

The contour maps for the polarization density $\Delta n(\mathbf{r})$ of the benzene due to the average potential $\tilde{\mathbf{V}}_{pc}$ are presented in Figure 2. $\Delta n(\mathbf{r})$ is constructed by subtracting the density n_0 of the solute at isolation from the distribution $\tilde{n}$ corresponding to the potential $\tilde{\mathbf{V}}_{pc}$. The upper figure illustrates the polarization on the molecular plan, which clearly shows the decrease in the

DOI: 10.1021/ct501133u
J. Chem. Theory Comput. 2015, 11, 1181−1194

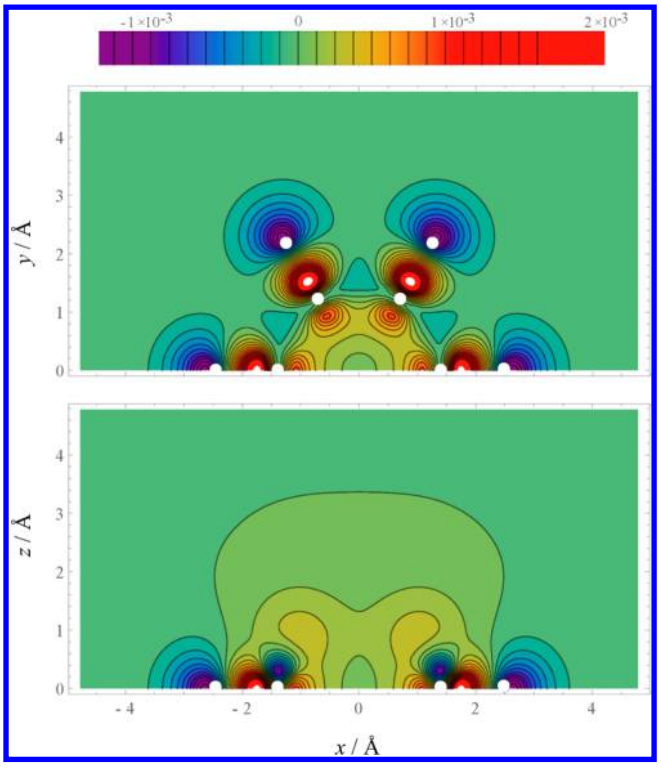

Figure 2. Contour plot of the electronic polarization density $\Delta n(\mathbf{r}) = \tilde{n} - n_0$ for benzene. The values of the density in legend are in the unit of au^{-3}. For the symmetry of benzene $\Delta n(\mathbf{r})$ is yielded by taking the average of the raw data of $\Delta n(\mathbf{r})$ with respect to the three symmetry planes, which are perpendicular to the x, y, and z axes. The other settings for graphics are the same as those described for Figure 1.

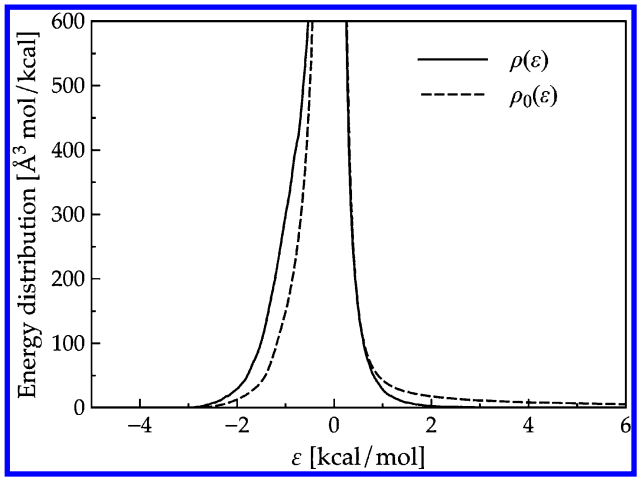

Figure 3. Two-body energy distribution functions $\rho(\varepsilon)$ and $\rho_0(\varepsilon)$ in solution and reference systems, respectively, for benzene with electron density $\tilde{n}$ in water. Note that the distributions are normalized by the number density of bulk water.

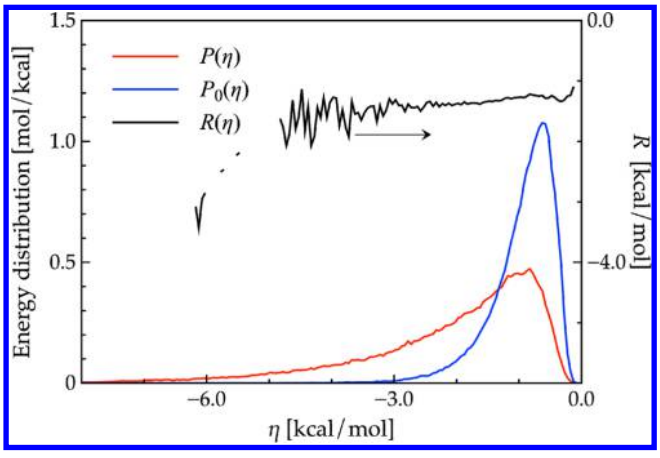

Figure 4. Distribution functions $P(\eta)$ and $P_0(\eta)$ of the polarization energy of benzene in solution and reference systems, respectively. $R(\eta)$ defined in eq 19 is also shown in the figure.

electron density at hydrogen atoms as a direct consequence of the positive potential surrounding the benzene ring. Instead, we found the electron population increases around the carbon atoms. Actually, the average of the ESP charge evaluated at carbon atom increases from 0.118 e at isolation to 0.132 e in the solution. In the lower panel of Figure 2, we observe that the electron density increased in the region above the benzene ring in consistent with the negative potential shown in Figure 1. The broadness of the increased density $\Delta n(\mathbf{r})$ above the ring can be attributed to the delocalized nature of the π electrons over the out-of-plane region.

The free energy contribution $\Delta\bar{\mu}$ defined in eq 15 for the solute with the fixed electron density $\tilde{n}$ was computed by means of the theory of energy representation, where the two-body energy distribution functions serve as fundamental variables. Figure 3 shows the energy distributions $\rho(\varepsilon)$, and $\rho_0(\varepsilon)$ for the solution and the reference systems, respectively. We observe a distinct peak around $\varepsilon = \sim 0$ kcal/mol of the energy coordinate for these functions. However, no other peak is found even in the solution system suggesting the weak solute−solvent interaction. We note that the potential $\tilde{\mathbf{V}}_{pc}$ and, consequently, the electron density $\tilde{n}$ are symmetric with respect to the symmetry plane of benzene. Hence, the solute with the density $\tilde{n}$ has no dipole moment. The free energy $\Delta\bar{\mu}$ due to two-body interaction was computed as $\Delta\bar{\mu} = +0.84$ kcal/mol by utilizing eq 12 in ref 39, which includes the distortion energy $E_{dist}[\tilde{n}] = +0.33$ kcal/mol associated with the potential $\tilde{\mathbf{V}}_{pc}$ and the long-range correction[81] $\Delta\bar{\mu}_{lc} = -0.45$ kcal/mol. Thus, the solvation free energy $\Delta\bar{\mu}$ of benzene with static polarization was found to be positive and could not realize the negative value of −0.87 kcal/mol given in an experiment.

4.2. Role of Dynamic Polarization in Hydration of Benzene. Figure 4 shows the distribution functions $P(\eta)$ and $P_0(\eta)$ for the solution and the reference systems, respectively, for benzene. It is recognized that the distribution $P(\eta)$ has large population on lower energy coordinate compared with $P_0(\eta)$. As defined in eq 18, the configuration sampling for the solvent in reference system is taken for the solute with the fixed electron density polarized under the potential $\tilde{\mathbf{V}}_{pc}$ shown in Figure 2. On the contrary, in the solution system, the solvent water molecules fully couple with the fluctuating electron density of the solute, where an induced dipole moment of the solute will make strong interactions with fractional charges on water molecules. Hence, the polarization energy η in the solution system has a longer tail in its distribution than that in the reference system. The distribution of the reference is narrow, and its range of the energy η is within $-3.0 \le \eta \le 0.0$ kcal/mol, showing a clear contrast to the broad distribution of the solution system. Thus, Figure 4 directly suggests the importance of the electron density fluctuation in hydration of

DOI: 10.1021/ct501133u
J. Chem. Theory Comput. 2015, 11, 1181−1194

benzene. Substituting these distribution functions into eq 19, we obtain the free energy $\delta\mu$ = −1.30 kcal/mol due to the electron density fluctuation. $R(\eta)$ presented in the figure is the function defined in eq 19, and it should be a constant function at the convergence of the distribution functions. $R(\eta)$ in Figure 4 shows a sound constancy with respect to the coordinate η. Summation of the two-body ($\Delta\bar{\mu}$) and many-body ($\delta\mu$) contributions leads to total solvation free energy $\Delta\mu$ of −0.47 kcal/mol, though it is slightly larger than the experimental value (−0.87 kcal/mol). It was, thus, demonstrated that the fluctuation of the electron density in response to the solvent dynamics play an essential role in the hydration of benzene. It is also interesting to compare the hydration free energy of benzene with that of cyclohexane. The experimental hydration free energy of cyclohexane is distinctly positive (1.230 kcal/mol).[31] The difference in the affinities of these aromatic solutes to the polar solvent can be apparently attributed to the existence of a few π electrons in benzene.

4.3. Decomposition of the Free Energy Due to Electron Density Fluctuation. As shown in eq 20, within the framework of the PT2 approach, it is straightforward to decompose the polarization energy $E'^{(2)}$ into the contributions $E'^{(2)}_{\pi}$ and $E'^{(2)}_{\sigma}$, respectively, from π and σ electrons. The distribution functions $P_{\pi}(\eta)$ and $P_{0,\pi}(\eta)$ of $E'^{(2)}_{\pi}$ in solution and reference systems, defined, respectively, in eqs 24 and 25, are drawn in Figure 5. The corresponding distributions $P_{\sigma}(\eta)$ and

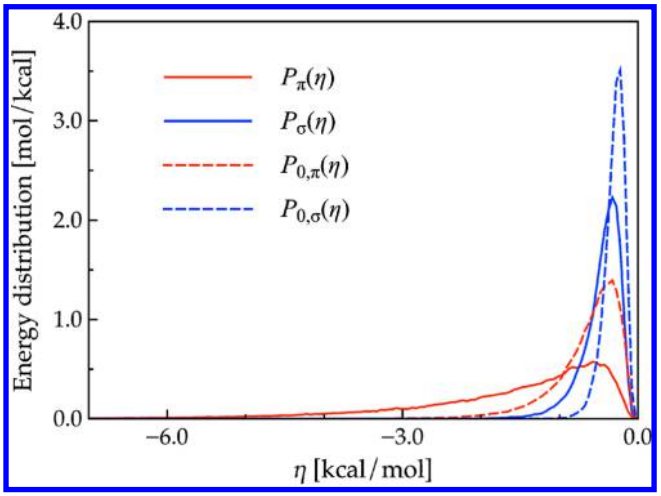

Figure 5. Distribution functions of the polarization energy η of benzene in water solution. $P_{\pi}(\eta)$ and $P_{0,\pi}(\eta)$ refer, respectively, the distributions for π electrons in solution and reference systems, while $P_{\sigma}(\eta)$ and $P_{0,\sigma}(\eta)$ refer those for σ electrons.

$P_{0,\sigma}(\eta)$ for σ electrons are also presented. It is recognized in the figure that the distributions for the solution systems are much broader than those for the corresponding references. This is because the configuration sampling in solution system is performed under the situation where the solvent fully couples with the fluctuating electron density of the solute. More importantly, the distributions for π electrons have longer tails in low energy coordinate than those for the σ electrons suggesting the stronger interactions of π electrons with water molecules. By inserting the distribution functions $P_{\pi}(\eta)$ and $P_{0,\pi}(\eta)$ to eq 23, we evaluated the free energy contribution arising from the fluctuation of π electrons as $\delta\mu_{\pi}$ = −0.94 kcal/mol. The contribution from σ electrons was also obtained as $\delta\mu_{\sigma}$ = −0.35 kcal/mol with the same procedure. The free energy components for benzene are summarized in the second row of Table 1. Thus, quantitative evaluation of the free energy

Table 1. Hydration Free Energies $\Delta\mu$ for Benzene and PME, and Their Components in Units of kcal/mol[a]

solute	$\Delta\bar{\mu}$	$\delta\mu$	$\delta\mu_{\sigma}$	$\delta\mu_{\pi}$	$\Delta\mu$	$\Delta\mu_{\text{expt.}}$[b]
benzene	0.84	−1.30	−0.35	−0.94	−0.47	−0.87
PME	−0.13	−1.71	−0.48	−1.08	−1.84	−1.04

[a] $\delta\mu$ was computed using eq 19, while its components $\delta\mu_{\sigma}$ and $\delta\mu_{\pi}$ were obtained with an approximate functional in eq (27. $\Delta\mu$ is given by the sum of $\Delta\bar{\mu}$ and $\delta\mu$. [b] Experimental values presented in ref 31.

components was made possible by means of the PT2 approach combined with the theory of solutions in energy representation. We note, however, that we employed an approximate functional of eq 27 to perform integration of $\omega(\eta;\lambda)$ in eq 23; hence, the individual values of $\delta\mu_{\pi}$ and $\delta\mu_{\sigma}$ are approximate. On the contrary, eq 19 includes no approximation and the total free energy value $\delta\mu$ is numerically exact. As described in the previous subsection, $\delta\mu$ was obtained as−1.30 kcal/mol using eq 19, which shows an excellent agreement with the sum of the approximate values $\delta\mu_{\pi}$ + $\delta\mu_{\sigma}$ = −1.29 kcal/mol. This substantiates the robustness of the functional of eq 27 and also the soundness of the free-energy decomposition analysis developed in the present work. The contribution of the π electrons to the free energy due to dynamic polarization was, thus, found to be ∼3 times as large as that of the σ electrons although the number of π electrons in benzene is only 3 and much less than that of σ electrons.

It is also of our concern to decompose the free energy $\delta\mu$ into the contributions due to the electron density fluctuations that are parallel (in-plane) and perpendicular (out-of-plane) to the molecular plane of benzene. Hereafter, we refer to these free energies as $\delta\mu_{\text{in}}$ and $\delta\mu_{\text{out}}$. Modifying eq 20 it is possible to introduce naturally the energy coordinates $E'^{(2)}_{\text{in}}$ and $E'^{(2)}_{\text{out}}$ responsible for these free energies, thus,

$$E'^{(2)} = E'^{(2)}_{\text{in}} + E'^{(2)}_{\text{out}} = \{(\sum_{i\in\sigma}^{\text{occ}}\sum_{a\in\sigma}^{\text{vir}} + \sum_{i\in\pi}^{\text{occ}}\sum_{a\in\pi}^{\text{vir}}) + (\sum_{i\in\sigma}^{\text{occ}}\sum_{a\in\pi}^{\text{vir}} + \sum_{i\in\pi}^{\text{occ}}\sum_{a\in\sigma}^{\text{vir}})\} \times \frac{1}{\varepsilon_i'^{(0)} - \varepsilon_a'^{(0)}} |\langle\varphi_i'^{(0)}|\mathbf{V}'_{\text{pc}}[\mathbf{X}]|\varphi_a'^{(0)}\rangle|^2 \quad (28)$$

It can be readily recognized that the electronic transitions $\sigma \rightarrow \sigma^*$ and $\pi \rightarrow \pi^*$ give rise to the polarization parallel to the molecular plane, while $\sigma \rightarrow \pi^*$ and $\pi \rightarrow \sigma^*$ transitions induce the out-of-plane polarization. Hence, the first and second terms in the right-hand side of the second equality in eq 28 constitute the energy of $E'^{(2)}_{\text{in}}$, and the third and fourth ones correspond to $E'^{(2)}_{\text{out}}$. The distribution functions are, then, constructed for $E'^{(2)}_{\text{in}}$ and $E'^{(2)}_{\text{out}}$ to evaluate the free energies $\delta\mu_{\text{in}}$ and $\delta\mu_{\text{out}}$, respectively. The result of the free energy decompositions is summarized in Table 2. It may be naturally expected that $\delta\mu_{\text{out}}$ dominates $\delta\mu$, because the benzene−water dimer favors the configuration where OH bond is pointing to the center of the aromatic ring. However, we found in the table that in-plane contribution $\delta\mu_{\text{in}}$ (−0.99 kcal/mol) dominates the free energy $\delta\mu$ for benzene. More explicitly, the free energy $\delta\mu_{\pi-\pi^*}$ (−0.76 kcal/mol) due to the polarization originating from the π−π^* transition gives the major contribution. The polarization along the molecular plane will be preferred in a condensed environment since it yields a large dipole moment as compared with the out-of-plane polarization.

DOI: 10.1021/ct501133u
J. Chem. Theory Comput. 2015, 11, 1181−1194

Table 2. Free Energies $\delta\mu$ Due to the Electron Density Fluctuation for Benzene and PME and Their Components in Units of kcal/mol[a]

		$\delta\mu_{in}$		$\delta\mu_{out}$	
solute	$\delta\mu$	$\delta\mu_{\pi-\pi^*}$	$\delta\mu_{\sigma-\sigma^*}$	$\delta\mu_{\pi-\sigma^*}$	$\delta\mu_{\sigma-\pi^*}$
benzene	−1.30	−0.99		−0.31	
		−0.76	−0.22	−0.18	−0.13
PME	−1.71	−1.17		−0.35	
		−0.87	−0.35	−0.21 −	0.12

[a] $\delta\mu$ was computed using eq 19, while their components $\delta\mu_{in}$, $\delta\mu_{out}$, $\delta\mu_{\pi-\pi^*}$, and $\delta\mu_{\sigma-\sigma^*}$ were obtained with an approximate functional in eq 27.

We make some remarks about the effects of the adopted force field or the level of theory in quantum chemical calculation on the present results. Because the electrostatic interaction between solute and solvent constitutes the major contribution to the free energy $\delta\mu$ the choice of the fractional charges on the MM water molecule would affect the values of $\delta\mu$ and their components. Our previous QM/MM-ER simulations revealed, however, that the solvation free energy[40] of a QM water in the SPC/E water solvent was in good agreement with that provided[39] with the TIP4P solvent (SPC/E, −6.9 kcal/mol; TIP4P, −7.0 kcal/mol) although the fractional charges specified in SPC/E model substantially differ from that in TIP4P. Thus, we speculate model dependence of $\delta\mu$ might not be serious in the practice. On the other hand, the two-body contribution $\Delta\bar{\mu}$ would be rather sensitive to the choice of the size parameters of a solute since the cavitation free energy of the solute is included in $\Delta\bar{\mu}$. In ref 70, we also examined the effect of the GGA (generalized gradient approximation) functional on the hydrogen bond (HB) curve of a water dimer represented with a QM/MM model. We found that HB energy evaluated with non-GGA functional adequately reproduces the GGA result, though it is well-known that GGA is essential for the sound description of the HB of water dimer whole of which is treated with DFT. Thus, we speculate that the present results deserve for quantitative discussions to a certain extent, though some of them should be carefully assessed in the future work.

4.4. Substituent Effect (Hydration of PME). Here, we investigate substituent effects on the hydration of a π-electron system. Methoxy group (CH_3O-) is known as a strong electron-donating group (EDG). Hence, it is expected that the introduction of a methoxy group to benzene as a substituent stabilizes the electron-resonating structures, which may increase the number of π electrons as a result. Indeed, it is increased from 3 to 5 when the solute is displaced from benzene to phenyl-methyl ether (PME: $CH_3O-C_6H_5$). These five orbitals

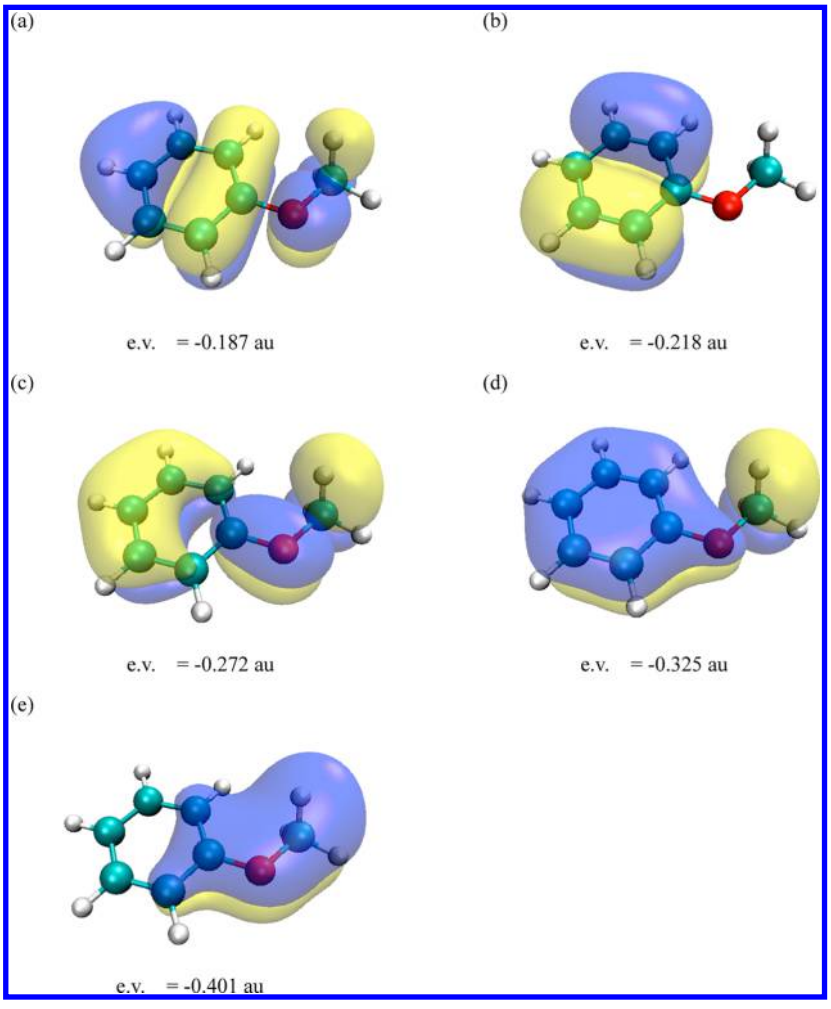

Figure 6. (a−e) Three-dimensional contour surfaces for the five π orbitals in phenyl methyl ether (PME) placed in a average potential $\tilde{\mathbf{V}}_{pc}$. The eigen value of each orbital is also presented under the figure. The isovalues of the contour surfaces are ±0.02 au.

DOI: 10.1021/ct501133u
J. Chem. Theory Comput. 2015, 11, 1181−1194

are depicted in Figures 6a−e. It is clearly shown that the wave functions on benzene are mixed with those in methoxy group to form new π orbitals delocalized over the system.

The average potential $\tilde{V}_{pc}$ was also build for PME in water solution through 500 ps simulation and the corresponding electron density $\tilde{n}$ was produced. Then, the distribution functions of pairwise interaction potential for the solute with $\tilde{n}$ were constructed to calculate the free energy $\Delta\overline{\mu}$ due to the two-body interaction. The energy distribution functions $\rho(\varepsilon)$ in solution and $\rho_0(\varepsilon)$ in reference systems for PME are presented in Figure 7. The hydration free energy of PME and its

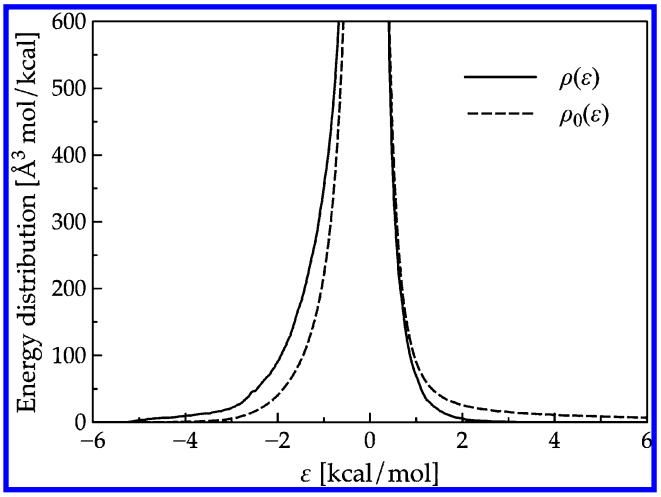

Figure 7. Two-body energy distribution functions $\rho(\varepsilon)$ and $\rho_0(\varepsilon)$ in solution and reference systems, respectively, for phenyl methyl ether (PME) with electron density $\tilde{n}$ in water. Note that the distributions are normalized by the number density of bulk water.

components are summarized in the third row of Table 1.It is apparent in Figure 7 that the distributions for PME have a large population on the low energy coordinate as compared to those for benzene shown in Figure 3. This can be attributed to the larger affinity of PME to water molecules than benzene. Indeed, the ESP charge at the oxygen atom of PME with density $\tilde{n}$ was evaluated as −0.55 e and that at the adjacent carbon atom in the benzene ring was obtained as +0.65 e exhibiting a large electronic polarization. Consequently, the free energy $\Delta\overline{\mu}$ of PME becomes negative, $\Delta\overline{\mu}$ = −0.13 kcal/mol, which includes the long-range correction $\Delta\overline{\mu}_{1c}$ = −0.59 kcal/mol. This is in contrast to the positive value of the free energy $\Delta\overline{\mu}$ for benzene (+0.83 kcal/mol). Thus, it was revealed that the static polarization in PME plays a role in the hydration process though not sufficient to reproduce the experimental value of $\Delta\mu_{expt.}$ = −1.04 kcal/mol. A notable feature in Figure 8 is that the distribution in solution has a longer tail over the low energy coordinate as compared with that for benzene in Figure 4. The distribution of PME in solution has a notable population even in the energy region of η < −9 kcal/mol, while that for benzene is completely vanished in the region. This can be attributed to the difference in the polarizabilities of these molecules. Using eq 19 the free energy $\delta\mu$ due to the density fluctuation was computed as −1.71 kcal/mol. The total solvation free energy $\Delta\mu$ of PME was, thus, given as −1.84 kcal/mol, though it is lower than the experimental value (−1.04 kcal/mol). The contribution of the dynamic polarization to hydration is, thus, enhanced by the introduction of the methoxy group to benzene. However, this is rather a matter of course, because

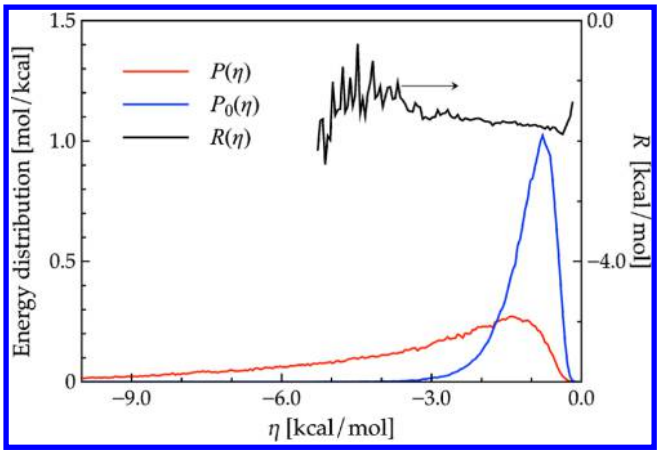

Figure 8. Distribution functions $P(\eta)$ and $P_0(\eta)$ of the polarization energy of phenyl methyl ether (PME) in solution and reference systems, respectively. $R(\eta)$ defined in eq 19 is also shown.

the number of electrons is increased when a hydrogen atom in benzene is replaced by a methoxy group.

To compute free energy contribution $\delta\mu$ due to the electron density fluctuation of PME, the distribution functions $P(\eta)$ and $P_0(\eta)$ are constructed in the solution and the reference systems, respectively. These functions are presented in Figure 8.

Presented in Figure 9 are the distribution functions $P_\pi(\eta)$ and $P_{0,\pi}(\eta)$ of the energy $E_\pi'^{(2)}$, which are for the solution and

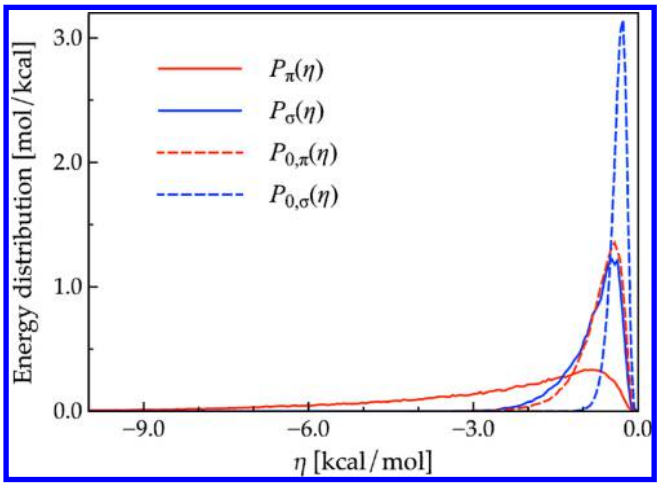

Figure 9. Distribution functions of the polarization energy η of phenyl methyl ether (PME) in water solution. $P_\pi(\eta)$ and $P_{0,\pi}(\eta)$ refer, respectively, the distributions for π electrons in solution and reference systems, while $P_\sigma(\eta)$ and $P_{0,\sigma}(\eta)$ refer those for σ electrons.

reference systems, respectively. The distributions $P_\sigma(\eta)$ and $P_{0,\sigma}(\eta)$ of $E_\sigma'^{(2)}$ are also drawn in the figure. A notable feature in these functions is the long-tail nature of the $P_\pi(\eta)$ on the lower energy coordinate, which is a common trend in the distributions for benzene, as is shown in Figure 5. $P_\pi(\eta)$ of PME has a larger population on the low energy coordinate compared to that of benzene, indicating the larger fluctuation of the π electrons in PME than benzene. As a result the contribution $\delta\mu_\pi$ due to the fluctuation of π electrons to the solvation, free energy was evaluated as −1.08 kcal/mol, slightly lower than that of benzene (−0.94 kcal/mol). These are, of course, due to the increase in the number of π electrons. For the σ electrons, the free energy contribution $\delta\mu_\sigma$ was computed

DOI: 10.1021/ct501133u
J. Chem. Theory Comput. 2015, 11, 1181−1194

Table 3. Hydration Free Energies $\Delta\mu$ for Ethene and 1,3-Butadiene, and Their Components in Units of kcal/mol[a]

	$\Delta\bar{\mu}$	$\delta\mu$	$\delta\mu_\sigma$	$\delta\mu_\pi$	$\Delta\mu$	$\Delta\mu_{expt.}$
ethene	2.32	−0.44 (±0.01)	−0.21 (±0.01)	−0.23 (±0.01)	1.88	1.27
1,3-butadiene	2.72	−1.24 (±0.11)	−0.38 (±0.03)	−0.76 (±0.09)	1.48	0.60

[a] $\delta\mu$ was computed using eq 19, while its components $\delta\mu_\sigma$ and $\delta\mu_\pi$ were obtained with an approximate functional in eq 27. $\Delta\mu$ is given by the sum of $\Delta\bar{\mu}$ and $\delta\mu$. Experimental values presented in ref 31. The values in the parentheses are the standard deviations.

as −0.48 kcal/mol, which is lower than the value for benzene (−0.35 kcal/mol). The decrease in the free energy $\delta\mu_\sigma$ can also be attributed to the increase in the number of σ electrons associated with the substitution. It is, however, interesting to note that the degree of stabilization in the free energy $\delta\mu_\sigma$ is comparable to that of $\delta\mu_\pi$ though the increase in the number of σ electrons on the substitution is much larger than that of π electrons. These free energy components reasonably reflect the difference in the softness of the π and σ electrons. We, thus, confirmed that the present analysis is adequate to evaluate reasonably the free energy components originating from the fluctuations of π and σ electrons in a QM solute in solution. It should also be noted that the sum of $\delta\mu_\sigma$ and $\delta\mu_\pi$ for PME is noticeably smaller than the value of $\delta\mu$ given by an exact functional. This is presumably because of the poor overlap between the distributions $P_\pi(\eta)$ and $P_{0,\pi}(\eta)$ for PME.

4.5. Delocalization Effect on Hydration. Hydration of a benzene molecule is also related to that of other π-conjugated systems. We consider here the effect of the length of π-conjugation on the hydration free energy. Elongation of the length of a π conjugated molecule stabilizes the orbital energies of the π electrons and also decreases the $\pi-\pi^*$ gap, which is often referred to as the delocalization effect in π electrons. This effect has a relevance to an experimental observation that the affinity of 1,3-butadiene (C_4H_6) to water solvent is larger than ethene (C_2H_4). That is, the hydration free energy of butadiene is experimentally given as 0.60 kcal/mol, being lower than that of ethene (1.27 kcal/mol) irrespective of its larger cavity volume. In this subsection, we address the issue of the delocalization effects on the hydration by performing the free energy decomposition analyses for ethene and 1,3-butadiene molecules. The solvation free energies and their components are summarized in Table 3. The two-body contribution $\Delta\bar{\mu}$ for ethene was computed as 2.32 kcal/mol and found to be smaller than that for butadiene (2.72 kcal/mol). The distribution functions from which these free energies were obtained are presented in the Supporting Information. The positively larger value $\Delta\bar{\mu}$ of butadiene than that of ethene may be attributed mainly to the larger exclusion volume of butadiene.

In the computation of the free energy $\delta\mu$ and their components, we performed 4 sets of 100 ps simulation to evaluate standard deviations. The free energy $\delta\mu$ was evaluated as the average of the free energies obtained from these 4 sets. The graphs of the distribution functions needed to construct the free energies $\delta\mu$ and their components are also given in the Supporting Information. Using eq 19, the free energy $\delta\mu$ was evaluated as −1.24 kcal/mol for butadiene and −0.44 kcal/mol for ethene. Thus, the absolute of the free energy $\delta\mu$ for butadiene was found to be about 3 times as large as that for ethene, suggesting the larger electronic fluctuation in butadiene compared to ethene. The decomposition of $\delta\mu$ using the approximate functional of eq 27 revealed that the contribution $\delta\mu_\sigma$ for butadiene is −0.38 kcal/mol, which is about two times as large as that for ethene (−0.21 kcal/mol). Of course, this is merely because the number of σ electrons in butadiene is almost twice as large as that in ethene. Interestingly, the free energy $\delta\mu_\pi$ for π electrons shows a clear contrast to σ electrons. That is, $\delta\mu_\pi$ for butadiene was computed as −0.76 kcal/mol, while that for ethene was −0.23 kcal/mol. Thus, it was found that $\delta\mu_\pi$ is about 3 times as large as that for ethylene. This is nothing but a consequence of the delocalization of the π electrons in a conjugated system. Approximately, −0.30 kcal/mol can be regarded as the free energy gain due to the delocalization of the π electrons. In fact, the HOMO−LUMO gap of butadiene and ethene was computed as 0.199 au and 0.232 au, respectively, under their corresponding average potentials $\tilde{V}_{pc}$. Accordingly, the polarizability along the longitudinal direction (parallel to double bonds) of butadiene placed in the average potential $\tilde{V}_{pc}$ was computed as 87.8 au while that of ethene was 37.1 au. The larger affinity of butadiene to water than ethene is the implication of the delocalization of the π electrons. The total solvation free energy $\Delta\mu$ (= $\Delta\bar{\mu} + \delta\mu$) was computed as 1.48 kcal/mol for butadiene and 1.88 kcal/mol for ethene. These values slightly overestimate the experimental values, which may be attributed to the size parameter of the force field adopted to the QM solutes. It should be stressed, however, that the computational free energy difference between these molecules shows rather good agreement with that evaluated from the experiments. Thus, it was revealed on the quantitative basis that the large affinity of butadiene to water compared to ethene is due mainly to the delocalization effect of the π electrons.

The energy distribution functions for the construction of the free energies $\Delta\bar{\mu}$, $\delta\mu$, $\delta\mu_\pi$, and $\delta\mu_\sigma$ for ethene are presented in Figures 3, 4, and 5 in Supporting Information, while those for butadiene are shown in Figures 6, 7, and 8 of the Supporting Information.

In summary, the present analyses provides us insights into the role of the delocalization of π electrons in π-conjugated molecules on the hydration on the basis of quantitative analyses. Explicitly, the relative affinity of butadiene to ethene molecules for water solvent is evaluated utilizing the QM/MM-PT2 approach combined with a theory of solutions. Elongation of the π-conjugation leads the enhancement of the polarizability of the system, and consequently, it was revealed that the free energy contribution $\delta\mu_\pi$ due to the dynamic polarization of π electrons are increased.

5. CONCLUSIONS

In this work, we developed a novel method to analyze the free energy $\delta\mu$ due to the electron density fluctuation of a solute in solution to clarify the mechanism responsible for the negative hydration free energy of benzene. The method is based on the QM/MM-ER approach combined with the second-order perturbation theory (PT2) developed in our previous work. With the PT2 framework, the polarization energy of the solute can be readily decomposed into the contributions due to the σ and π electrons. Then, it becomes quite straightforward to formulate the Kirkwood's charging equations which define individual free energies $\delta\mu_\sigma$ and $\delta\mu_\pi$ due, respectively, to the σ

DOI: 10.1021/ct501133u
J. Chem. Theory Comput. 2015, 11, 1181−1194

and π electrons. By virtue of the approximate functional in the energy representation, $\delta\mu_\sigma$ and $\delta\mu_\pi$ can be evaluated in terms of the distribution functions of the polarization energies associated with the fluctuations of σ and π electrons.

We first define the static polarization as the distortion of a solute's electron density under the influence of the average electric field $\tilde{V}_{pc}(\mathbf{r})$ yielded by solvent. In this work, we focus our attention on the dynamic polarization defined as the residual distortion of the electron density due to the instantaneous electric field $V_{pc}(\mathbf{r}) - \tilde{V}_{pc}(\mathbf{r})$. For the benzene−water system, the hydration free energy $\Delta\bar{\mu}$ due to the static polarization was obtained as +0.83 kcal/mol. Thus, we found the static polarization does not realize the negative hydration free energy of benzene. It was revealed, however, inclusion of the free energy $\delta\mu$ (= −1.30 kcal/mol) due to the electron density fluctuation around the fixed density led to a negative solvation free energy of −0.47 kcal/mol suggesting the importance of the dynamic polarization in the hydration of aromatic molecules. Further, the decomposition of the free energy $\delta\mu$ revealed that the contribution $\delta\mu_\pi$ (= −0.94 kcal/mol) due to the π electrons dominates the total free energy $\delta\mu$. Thus, the role of the π electrons in hydration was reasonably quantified by means of the QM/MM-ER approach combined with PT2. In addition, the free energy $\delta\mu$ was decomposed into the contribution due to "in-plane" and "out-of-plane" polarization of the electron density. We found that the dynamic polarization of electrons along the molecular plane, that is mainly attributed to the HOMO−LUMO transition ($\pi \rightarrow \pi^*$ transition), dominates the free energy $\delta\mu$.

The substituent effect on the hydration was also examined by carrying out the same analysis. Introduction of a strong electron-donating group (CH_3O) to benzene increases the number of π-electrons from 3 to 5 since the methoxy group stabilizes electron-resonating structures. Accordingly, the free energy $\delta\mu_\pi$ for PME was obtained as −1.04 kcal/mol, being lower than that for benzene (−0.94 kcal/mol). The free energy $\delta\mu_\sigma$ for PME (−0.48 kcal/mol) was also found to be lower than that for benzene (−0.35 kcal/mol) due to the increase in the number of σ electrons. Thus, the substituent effects on the individual free energy contributions were reasonably evaluated through the decomposition analyses.

The delocalization effects of π electrons on the hydration free energies were also investigated with the same analyses for the free energies $\delta\mu$ of ethene and 1,3-butadiene in water solutions. The free energy $\delta\mu_\sigma$ for butadiene was computed as −0.38 kcal/mol and found to be almost as twice as that for ethene (−0.19 kcal/mol) merely as a consequence of the fact that butadiene has twice the number of σ electrons of ethene. In contrast, the free energy contribution $\delta\mu_\pi$ for butadiene was obtained as −0.76 kcal/mol, which is about three times as large as that for ethene (−0.26 kcal/mol). Because the elongation of a π-conjugated polyacetylene chain leads to enhancement of the polarizability of the π electrons, the free energy $\delta\mu_\pi$ of each π orbital will be lowered when the solute is displaced from ethene to butadiene by adding a polyacetylene unit. Thus, we clarify the mechanism that 1,3-butadiene has low solvation free energy (0.60 kcal/mol) as compared to ethene (1.27 kcal/mol).

APPENDIX: DERIVATION OF EQUATION 22

Here, we derive the Kirkwood's charging equation in energy representation for the free energy $\delta\mu_\pi$ due to fluctuation of π electrons in a π conjugated system. We start from the right-hand side of the second equality of eq 21.

$$\delta\mu_\pi = \int_0^1 d\lambda \int d\mathbf{X}\rho(\mathbf{X};\lambda)\frac{d}{d\lambda}E'^{(2)}_{\pi,\lambda}[\mathbf{X}] \tag{A1}$$

As described in the text, the notation $\mathbf{X}$ in eq A1 collectively represents the configuration of the solvent molecules. For arbitrary different configurations $\mathbf{X}_A$ and $\mathbf{X}_B$ which satisfy

$$E'^{(2)}_{\pi}[\mathbf{X}_A] = E'^{(2)}_{\pi}[\mathbf{X}_B] \tag{A2}$$

we consider a subset of potentials $\{E'^{(2)}_{\pi,\lambda}\}$ that satisfies the relation

$$E'^{(2)}_{\pi,\lambda}[\mathbf{X}_A] = E'^{(2)}_{\pi,\lambda}[\mathbf{X}_B] \tag{A3}$$

irrespective of the choice of the coupling parameter λ ($0 \le \lambda \le 1$). Employing the potentials in this subset we obtain the transformation for eq A1, thus,

$$\begin{aligned}\delta\mu &= \int_0^1 d\lambda \int d\mathbf{X}\rho(\mathbf{X};\lambda)\frac{d}{d\lambda}E'^{(2)}_{\lambda}[\mathbf{X}] \\ &= \int_0^1 d\lambda \int d\eta \int d\mathbf{X}\delta(\eta - E'^{(2)}_{\lambda}[\mathbf{X}])\rho(\mathbf{X};\lambda)\frac{d}{d\lambda}E'^{(2)}_{\lambda}[\mathbf{X}] \\ &= \int_0^1 d\lambda \int d\eta\rho^e(\eta;\lambda)\frac{d}{d\lambda}E'^{(2),e}_{\lambda}(\eta)\end{aligned} \tag{A4}$$

where the energy distribution function $\rho^e(\eta;\lambda)$ is defined as

$$\rho^e(\eta;\lambda) = \int d\mathbf{X}\delta(\eta - E'^{(2)}_{\lambda}[\mathbf{X}])\rho(\mathbf{X};\lambda) \tag{A5}$$

Note that the suffix π are dropped for brevity in eqs A4 and A5. $\rho^e(\eta;1)$ in eq A5 is the same as the distribution defined by eq 24. Thus, we obtain the Kirkwood's charging equation (eq 22) in energy representation for $\delta\mu_\pi$. The formulation for the free energy $\delta\mu_\sigma$ is, of course, completely parallel to that for $\delta\mu_\pi$.

ASSOCIATED CONTENT

Supporting Information

Additional figures and tables. This material is available free of charge via the Internet at http://pubs.acs.org/.

AUTHOR INFORMATION

Corresponding Author

*E-mail: hideaki@m.tohoku.ac.jp.

Notes

The authors declare no competing financial interest.

ACKNOWLEDGMENTS

This work is supported by the Grant-in-Aid for Scientific Research on Innovative Areas (No. 23118701) from the Ministry of Education, Culture, Sports, Science, and Technology (MEXT) and by the Grant-in-Aid for Challenging Exploratory Research (No. 25620004) from the Japan Society for the Promotion of Science (JSPS), and by the Nanoscience Program and the Computational Materials Science Initiative of the Next-Generation Supercomputing Project.

REFERENCES

(1) Hobza, P.; Müller-Dethlefs, K. *Non-covalent Interaction Theory and Experiment*; RSC Theoretical and Computational Chemistry Series: Cambridge, 2010.

(2) Warshel, A. *Computer Modeling of Chemical Reactions in Enzymes and Solutions*; Wiley: New York, 1991.

(3) Gao, J.; Xia, X. *Science* **1992**, *258*, 631−635.

DOI: 10.1021/ct501133u
J. Chem. Theory Comput. 2015, 11, 1181−1194

(4) *Structure and Reactivity in Aqueous Solution*; Cramer, C. J., Truhlar, D. G., Eds.; ACS Symposium Series; American Chemical Society: Washington, DC, 1994; Vol *568*.
(5) *Solvent Effects and Chemical Reactivity*; Tapia, O., Bertrán, J., Eds.; Kluwer Academic: Dordrecht, 1996.
(6) *Classical and Quantum Dynamics in Condensed Phase Simulations*; Berne, B. J., Ciccotti, G., Coker, D. F., Eds.; World Scientific: Singapore, 1998.
(7) Ruiz-López, M. F., Ed. Combined QM/MM Calculations in Chemistry and Biochemistry Special Issue*J. Mol. Struct.: THEOCHEM* **2003**, *632*, 1−336.
(8) Voth, G. A. *Acc. Chem. Res.* **2006**, *39*, 143−150.
(9) Hu, H.; Yang, W. *Annu. Rev. Phys. Chem.* **2008**, *59*, 573−601.
(10) Edited by Canuto, S. *Solvation effects on Molecules and Biomolecules: Challenges and Advances in Computational Chemistry and Physics*; Springer: Heidelberg, 2008, Vol *6*.
(11) Edited by Canuto, S. *Combining Quantum Mechanics and Molecular Mechanics: Some Recent Progresses in QM/MM Methods, Advances in Quantum Chemistry Vol. 59*; Elsevier: Amsterdam, 2010.
(12) Meyer, E. A.; Castellano, R. K.; Diederich, F. *Angew. Chem., Int. Ed.* **2003**, *39*, 1210−1250.
(13) Edited by Hobza, P. *Themed Issue on 'Stacking Interactions', Phys. Chem. Chem. Phys.* **2008**, *19*, 2561−2868.
(14) Nishio, M.; Umezawa, Y. *Bioorg. Med. Chem.* **1993**, *6*, 493−504.
(15) Dougherty, D. A. *Science* **1996**, *271*, 163−168.
(16) Ma, J. C.; Dougherty, D. A. *Chem. Rev.* **1997**, *97*, 1303−1324.
(17) Gallivan, J. P.; Dougherty, D. A. *Proc. Natl. Acad. Sci. U.S.A.* **1999**, *96*, 9459−9464.
(18) Gallivan, J. P.; Dougherty, D. A. *J. Am. Chem. Soc.* **2000**, *122*, 870−874.
(19) Tatko, C. D.; Waters, M. L. *J. Am. Chem. Soc.* **2004**, *126*, 2028−2034.
(20) Harigai, M.; Kataoka, M.; Imamoto, Y. *J. Am. Chem. Soc.* **2006**, *128*, 10646−10647.
(21) Tsuzuki, S.; Fujii, A. *Phys. Chem. Chem. Phys.* **2008**, *10*, 2584−2594.
(22) Sponer, J.; Riley, K. E.; Hobza, P. *Phys. Chem. Chem. Phys.* **2008**, *10*, 2595−2610.
(23) Hagiwara, Y.; Kang, J.; Tateno, M. *J. Chem. Theory Comput.* **2011**, *7*, 2593−2599.
(24) Jeffrey, G. A. *An Introduction to Hydrogen Bonding*; Oxford University Press: Oxford, 1997.
(25) Edited by Kuwajima, K. et al. *Water and Biomolecules*; Springer: Heidelberg, 2009.
(26) Gilli, G.; Gilli, P. *The Nature of the Hydrogen Bond: Outline of a Comprehensive Hydrogen Bond Theory*; Oxford University Press: Oxford, 2009.
(27) Nishio, M.; Hirota, M.; Umezawa, Y.; *The CH/π Interaction: Evidence, Nature, and Consequences*; Wiley: New York, 1998.
(28) Levitt, M.; Perutz, M. F. *J. Mol. Biol.* **1988**, *201*, 751−754.
(29) Suzuki, S.; Green, P. G.; Bumgarner, R. E.; Dasgupta, S.; Goddard, W. A., III; Blake, G. A. *Science* **1992**, *257*, 942−945.
(30) Tsuzuki, S.; Honda, K.; Uchimaru, T.; Mikami, M.; Tanabe, K. *J. Am. Chem. Soc.* **2000**, *122*, 11450−11458.
(31) Gallicchio, E.; Zhang, L. Y.; Levy, R. M. *J. Comput. Chem.* **2002**, *23*, 517−529.
(32) Ravishanker, G.; Mehrotra, P. K.; Mezei, M.; Beveridge, D. L. *J. Am. Chem. Soc.* **1984**, *106*, 4102−4108.
(33) Raschke, T. M.; Levitt, M. *Proc. Natl. Acad. Sci. U.S.A.* **2005**, *102*, 6777−6782.
(34) Schravendijk, P.; van der Vegt, N. F. A. *J. Chem. Theory Comput.* **2005**, *1*, 643−652.
(35) Yonezawa, Y.; Nakata, K.; Takada, T.; Nakamura, H. *Chem. Phys. Lett.* **2006**, *428*, 74−77.
(36) Graziano, G. *Chem. Phys. Lett.* **2006**, *429*, 114−118.
(37) Allesch, M.; Schwegler, E.; Galli, G. *J. Phys. Chem. B* **2007**, *111*, 1081−1089.
(38) Allesch, M.; Lightstone, F. C.; Schwegler, E.; Galli, G. *J. Chem. Phys.* **2008**, *128*, 014501.
(39) Takahashi, H.; Matubayasi, N.; Nakahara, M.; Nitta, T. *J. Chem. Phys.* **2004**, *121*, 3989−3999.
(40) Takahashi, H.; Omi, A.; Morita, A.; Matubayasi, N. *J. Chem. Phys.* **2012**, *136*, 214503.
(41) Matubayasi, N.; Nakahara, M. *J. Chem. Phys.* **2000**, *113*, 6070−6081.
(42) Matubayasi, N.; Nakahara, M. *J. Chem. Phys.* **2002**, *117*, 3605−3616; **2003**, *118*, 2446.
(43) Matubayasi, N.; Nakahara, M. *J. Chem. Phys.* **2003**, *119*, 9686−9702.
(44) Karino, Y.; Fedrov, M. V.; Matubayasi, N. *Chem. Phys. Lett.* **2010**, *496*, 351−355.
(45) Takahashi, H.; Satou, W.; Hori, T.; Nitta, T. *J. Chem. Phys.* **2005**, *122*, 044504.
(46) Takahashi, H.; Kawashima, Y.; Nitta, T.; Matubayasi, N. *J. Chem. Phys.* **2005**, *123*, 124504.
(47) Hori, T.; Takahashi, H.; Nakano, M.; Nitta, T.; Yang, W. *Chem. Phys. Lett.* **2005**, *419*, 240−244.
(48) Takahashi, H.; Tanabe, K.; Aketa, M.; Kishi, R.; Furukawa, S.; Nakano, M. *J. Chem. Phys.* **2007**, *126*, 084508.
(49) Hori, T.; Takahashi, H.; Furukawa, S.; Nakano, M.; Yang, W. *J. Phys. Chem. B* **2007**, *111*, 581−588.
(50) Takahashi, H.; Ohno, H.; Yamauchi, T.; Kishi, R.; Furukawa, S.; Nakano, M.; Matubayasi, N. *J. Chem. Phys.* **2008**, *128*, 064507.
(51) Takahashi, H.; Ohno, H.; Kishi, R.; Nakano, M.; Matubayasi, N. *Chem. Phys. Lett.* **2008**, *456*, 176−180.
(52) Takahashi, H.; Ohno, H.; Kishi, R.; Nakano, M.; Matubayasi, N. *J. Chem. Phys.* **2008**, *129*, 205103.
(53) Takahashi, H.; Miki, F.; Ohno, H.; Kishi, R.; Ohta, S.; Furukawa, S.; Nakano, M. *J. Math. Chem.* **2009**, *46*, 781−794.
(54) Takahashi, H.; Maruyama, K.; Karino, Y.; Morita, A.; Nakano, M.; Jungwirth, P.; Matubayasi, N. *J. Chem. Phys. B* **2011**, *115*, 4745−4751.
(55) Takahashi, H.; Iwata, Y.; Kishi, R.; Nakano, M. *Int. J. Quantum Chem.* **2011**, *111*, 1748−1762.
(56) Suzuoka, D.; Takahashi, H.; Morita, A. *J. Chem. Phys.* **2014**, *140*, 134111.
(57) Allen, L. C. *Phys. Rev.* **1960**, *118*, 167−175.
(58) Francl, M. M. *J. Phys. Chem.* **1985**, *89*, 428−433.
(59) Luque, F. J.; Orozco, M. *J. Comput. Chem.* **1998**, *19*, 866−881.
(60) Cubero, E.; Luke, F. J.; Orozco, M.; Gao, J. *J. Phys. Chem. B* **2003**, *107*, 1664−1671.
(61) Tomasi, J.; Mennucci, B.; Cammi, R. *Chem. Rev.* **2005**, *105*, 2999−3094.
(62) Hansen, P.; McDonald, I. R. *Theory of Simple Liquids*, 3rd ed.; Academic: London, 2006.
(63) Hohenberg, P.; Kohn, W. *Phys. Rev.* **1964**, *136*, B864−B871.
(64) Kohn, W.; Sham, L. J. *Phys. Rev.* **1965**, *140*, A1133−A1138.
(65) Parr, R. G.; Yang, W. *Density-Functional Theory of Atoms and Molecules*; Oxford University Press: New York, 1989.
(66) Chelikowsky, J. R.; Troullier, N.; Saad, Y. *Phys. Rev. Lett.* **1994**, *72*, 1240−1243.
(67) Chelikowsky, J. R.; Troullier, N.; Wu, K.; Saad, Y. *Phys. Rev. B* **1994**, *50*, 11355−11364.
(68) Takahashi, H.; Hori, T.; Wakabayashi, T.; Nitta, T. *Chem. Lett.* **2000**, *29*, 222−223.
(69) Takahashi, H.; Hori, T.; Wakabayashi, T.; Nitta, T. *J. Phys. Chem. A* **2001**, *105*, 4351−4358.
(70) Takahashi, H.; Hori, T.; Hashimoto, H.; Nitta, T. *J. Comput. Chem.* **2001**, *22*, 1252−1261.
(71) Ten-no, S.; Hirata, F.; Kato, S. *J. Chem. Phys.* **1994**, *100*, 7443−7453.
(72) Sato, H.; Hirata, F. *J. Phys. Chem. B* **1999**, *103*, 6596−6604.
(73) Sakuraba, S.; Matubayasi, N. *J. Chem. Phys.* **2011**, *135*, 114108.
(74) Dunning, T. H. *J. Chem. Phys.* **1989**, *90*, 1007−1023.
(75) Frisch, M. J.; Trucks, G. W.; Schlegel, H. B.; Scuseria, G. E.; Robb, M. A.; Cheeseman, J. R.; Scalmani, G.; Barone, V.; Mennucci, B.; Petersson, G. A.; Nakatsuji, H.; Caricato, M.; Li, X.; Hratchian, H. P.; Izmaylov, A. F.; Bloino, J.; Zheng, G.; Sonnenberg, J. L.; Hada, M.;

DOI: 10.1021/ct501133u
J. Chem. Theory Comput. 2015, 11, 1181−1194

Ehara, M.; Toyota, K.; Fukuda, R.; Hasegawa, J.; Ishida, M.; Nakajima, T.; Honda, Y.; Kitao, O.; Nakai, H.; Vreven, T.; Montgomery, J. A.; Peralta, Jr., J. E.; Ogliaro, F.; Bearpark, M.; Heyd, J. J.; Brothers, E.; Kudin, K. N.; Staroverov, V. N.; Keith, T.; Kobayashi, R.; Normand, J.; Raghavachari, K.; Rendell, A.; Burant, J. C.; Iyengar, S. S.; Tomasi, J.; Cossi, M.; Rega, N.; Millam, J. M.; Klene, M.; Knox, J. E.; Cross, J. B.; Bakken, V.; Adamo, C.; Jaramillo, J.; Gomperts, R.; Stratmann, R. E.; Yazyev, O.; Austin, A. J.; Cammi, R.; Pomelli, C.; Ochterski, J. W.; Martin, R. L.; Morokuma, K.; Zakrzewski, V. G.; Voth, G. A.; Salvador, P.; Dannenberg, J. J.; Dapprich, S.; Daniels, A. D.; Farkas, O.; Foresman, J. B.; Ortiz, J. V.; Cioslowski, J.; Fox, D. J. *Gaussian 09*, Revision C.01; Gaussian, Inc.: Wallingford CT, 2010.

(76) Becke, A. D. *Phys. Rev. A* **1988**, *38*, 3098−3100.

(77) Becke, A. D. *J. Chem. Phys.* **1993**, *98*, 5648−5652.

(78) Lee, C.; Yang, W.; Parr, R. G. *Phys. Rev. B* **1988**, *37*, 785−789.

(79) Kleinman, L.; Bylander, D. M. *Phys. Rev. Lett.* **1982**, *48*, 1425−1428.

(80) Ono, T.; Hirose, K. *Phys. Rev. Lett.* **1999**, *82*, 5016−5019.

(81) Allen, M. P.; Tildesley, D. J. *Computer Simulation of Liquids*; Oxford University Press: Oxford, 1987.

(82) Frenkel, D.; Smit, B. *Understanding Molecular Simulation*; Academic: London, 1996.

(83) Berendsen, H. J. C.; Grigera, J. R.; Straatsma, T. P. *J. Phys. Chem.* **1987**, *91*, 6269−6271.

(84) van Gunsteren, W. F.; Billeter, S. R.; Eising, A. A.; Hünenberger, P. H.; Krüger, P.; Mark, A. E.; Scott, W. R. P.; Tironi, I. G. *Biomolecular Simulation: The GROMOS96 Manual and User Guide*; vdf Hochschulverslag: ETH Zürich, Switzerland, 1996.

(85) Jorgensen, W. L.; Maxwell, D. S.; Tirado-Rives, J. *J. Am. Chem. Soc.* **1996**, *118*, 11225−11236.

DOI: 10.1021/ct501133u
J. Chem. Theory Comput. 2015, 11, 1181−1194